

06616

AISC E&R Library



7102

JMM 11/18
IMPORTANT
STUFF

973

~~HE~~
ROD
~~FB~~
~~SP~~



PMFSEL THESIS NO. 80-1
SEPTEMBER 1980

THE BEHAVIOR AND ANALYSIS OF
DOUBLE ROW BOLTED SHEAR
WEB CONNECTIONS

By

J. M. RICLES

and

J. A. YURA

Sponsored by

American Institute of Steel Construction

DEPARTMENT OF CIVIL ENGINEERING / Phil M. Ferguson Structural
Engineering Laboratory

THE UNIVERSITY OF TEXAS AT AUSTIN

RR973

7102

80617

THE BEHAVIOR AND ANALYSIS OF DOUBLE ROW
BOLTED SHEAR WEB CONNECTIONS

by

J. M. Ricles and J. A. Yura

This work has been carried out as a part of an investigation
sponsored by the American Institute of Steel Construction

Phil M. Ferguson Structural Engineering Laboratory
Department of Civil Engineering
The University of Texas at Austin
Austin, Texas 78758

September 1980

A C K N O W L E D G M E N T S

The results of one phase of the research project, Web Shear Connection Tests, sponsored by the American Institute of Steel Construction, are presented. The tests were conducted at the Phil M. Ferguson Structural Research Laboratory of The University of Texas at Austin. The computer analysis was done using the computer system at The University of Texas at Austin.

The author is indebted to Dr. Joseph A. Yura who supervised the research and was professor in charge of this thesis. The guidance of Dr. Peter C. Birkemoe, Dr. Jose M. Roesset, and Dr. C. P. Johnson is also greatly acknowledged. Special thanks is extended to Fereidoon Ghodsi and Bert G. Shelton who helped in all phases of the preparation and testing of the specimens. Sincere appreciation is given to George Moden, Dick Marshall, Daniel Perez and all the staff at the Phil M. Ferguson Laboratory. In addition, the help and cooperation of Mrs. Tina Robinson who typed the complete manuscript is greatly appreciated.

J.M.R.
September 1980

A B S T R A C T

The behavior of double row bolted shear connections was examined by conducting a series of eight full-scale tests and an elastic finite element analysis. The test program involved coped and uncoped beams with compact type connections where the full depth of the beam web was not developed by the connection. All of the specimens failed in a block shear mode.

The results of the tests indicate the 1978 AISC Specification formula for block shear resistance predicted higher capacities than actually obtained in the tests. Also, the current method of checking the bending stresses at the cope was found to be inadequate. A new recommendation for a block shear failure model is given.

TABLE OF CONTENTS

Chapter		Page
1	INTRODUCTION	1
2	TEST PROGRAM	8
	Test Specimens	8
	Test Setup	12
	Instrumentation	14
	Test Procedure	17
3	EXPERIMENTAL BEHAVIOR	18
4	FINITE ELEMENT ANALYSIS	37
	Purpose	37
	Description of Finite Element Model	37
	Finite Element Results	43
5	Discussion of Test Results and Design Recommendations .	58
	Effect of End and Edge Distance	58
	AISC Allowable Connection Capacity	61
	Considering the Effect of Eccentricity	64
	Connection Capacity Controlled by End or Edge Distance	65
	Block Shear	67
	Stability of the Web	72
6	SUMMARY AND CONCLUSIONS	76
	APPENDIX I LOAD-DEFORMATION CONNECTION BEHAVIOR	78
	APPENDIX II REPRESENTATIVE DIMENSIONS OF SPECIMENS	87
	APPENDIX III SAMPLE CALCULATIONS FOR TEST 18-12	89
	BIBLIOGRAPHY	93

LIST OF TABLES

Table	Page
2.1 Tensile Coupon Test Results Representing Heat 1 and Heat 2	11
5.1 AISC Allowable Reaction	62
5.2 1978 AISC Allowable Reaction Based on Block Shear . . .	68
5.3 Reaction Capacity Based on New Block Shear Failure Model	72
II-1 Average Representative Dimensions	88

LIST OF FIGURES

Figure	Page
1.1 Bearing stress equations plotted against data from lap splice tests (Ref. 4)	3
1.2 Test setup for uncoped specimen	4
1.3 Test setup for coped specimen	4
1.4 Failure of connection caused by fracturing along plane A-A and B-B	6
1.5 Block shear failure model	6
2.1a Detail of connection specimens from heat 1	9
2.1b Detail of connection specimens from heat 2	10
2.2 Test setup schematic	13
2.3 View of bracing system supporting the test frame and test beam	15
2.4 Closeup of bracing plates	15
2.5 Instrumentation at the connection	16
3.1 Connection reaction versus connection deflection	19
3.2 Connection reaction versus deflection of tension flange	20
3.3 Connection reaction versus net deflection of connection	21
3.4 Test 18-12 after failure	23
3.5 Flexure stresses caused by connection rotation about vertical plane	24
3.6 Applied load versus deflection at point of load	25
3.7 Moment developed at the connection versus rotation of clip angles	26
3.8 Plot of the location of the point of inflection versus the reaction at the connection	28
3.9 Reaction at the connection versus the rotation of the clip angles and the beam	29

Figure	Page
3.10 Yielding in the outstanding legs of the clip angles	30
3.11 Failed specimens	31
3.12 Location of yielding in the compression flange . . .	36
4.1 Finite element model of test beam	38
4.2 Enlarged view of the finite element model of the connection	39
4.3a Clip angle behavior	40
4.3b Clip angles pulling away from the column	40
4.4 Modeling of the clip angle	41
4.5a Stress contours from the finite element analysis . .	44
4.5b Yield lines in test specimen	44
4.6 Vertical stress distribution, case 1	45
4.7 Vertical stress distribution, case 2	45
4.8 Vertical stress distribution, case 3	46
4.9 Vertical stress distribution, case 4	46
4.10 Vertical stress distribution, case 5	47
4.11 Vertical stress distribution, case 6	47
4.12 Vertical stress distribution, case 7	48
4.13 Vertical stress distribution, case 8	48
4.14 Vertical stress distribution, case 9	49
4.15a Stress distribution for 1 in. end distance	53
4.15b Stress distribution for 2 in. end distance	53
4.16 Typical distribution of horizontal stresses	55
4.17 Finite element and beam theory bending stress distribution at the cope	56
5.1 Connection reaction versus net deflection at the connection for specimens of heat 1	59
5.2 Connection reaction versus net deflection at the connection for specimens of heat 2	60
5.3 Model for basis of bearing stress formula	66

Figure		Page
5.4	Area of web where fracture first occurs	69
5.5	New failure model for block shear	70
5.6	Top view of beam showing a buckle in the web at the cope	73
5.7	Compact connection placed at a lower depth	75

NOTATION

- A_b Projected area of bolt on bearing surface (dt_w)
- A_t Net area of web in tensile stress plane of connection
- A_v Net area of web in shear stress plane of connection
- A_w Area of web at the cope ($d_n t_w$)
- B Depth of outstanding legs of clip angles resisting flexure
- c Distance from neutral axis of beam cross section to fiber of which bending stress is calculated
- d Diameter of bolt
- d_h The effective diameter of the bolt hole ($d + 1/8$)
- d_n Depth of beam at the cope
- e Eccentricity at the connection (M/R)
- E Modulus of elasticity of steel (29000 ksi)
- e_g Edge distance from center line of the bolt hole to free edge
- e_n End distance from center line of the bolt hole to free end
- F_u Static ultimate tensile stress of material
- F_p Static bearing stress of material
- F_y Static yield stress of material
- g Gage length of bolt line
- I Moment of inertia
- K Spring constant stiffness equivalent to stiffness of outstanding leg of clip angle
- L Distance from center line of the bolt hole to the free edge

M	Moment in test beam or at the test connection
M_p	Plastic moment capacity of test beam
n	Number of bolts in test connection
P	Load carried by one bolt
P_b	Bolt shear force ignoring effect of eccentricity
P_g	Reaction based on top edge distance of connection $\left(\frac{e F t}{g u w}\right)_n$
P_n	Reaction based on end distance of connection $\left(\frac{e F t}{n u w}\right)_n$
P_p	Reaction based on bolt bearing force ($F_p A_b n$)
R	Reaction at test connection
R_{allow}	Allowable reaction of the test connection based on the 1978 AISC Specification
R_f	Ultimate capacity of test connection based on the new block shear failure model
R_{max} or R_u	Maximum reaction obtained by the test connection
s	<i>Center to center spacing of bolts</i>
t	Thickness of clip angles in test connection
t_w	Thickness of web of the test beam
V	Allowable AISC web shear ($0.4F_y A_w$)
V_b	Allowable bolt shear (26.5 kips for 3/4 in. diameter A325 bolts in double shear)
V_u	Shear yield capacity of test beam web $\left(A_w \frac{F_y}{\sqrt{3}}\right)$
Δ	Deflection

- Δ_1 Deflection of compression flange at the connection
 Δ_2 Deflection of tension flange at the connection
 ϕ Rotation of member
 σ Bending stress in test beam based on beam theory $\left(\frac{Mc}{I}\right)$
 τ_{avg} Average nominal shear stress at the connection based on
 finite element analysis $\left(\frac{R}{d_n t_w}\right)$

Both of these equations are plotted with test data in Fig. 1.1. Equation (1.2) becomes unconservative when the L/d ratio exceeds 3.0 hence the upper limit of the bearing ratio F_p/F_u was placed at 3.0. The 1976 RCRS Specification³ adopted these bearing strength recommendations using a factor of safety of 2.0 as:

$$F_p \leq \frac{LF_u}{2d} \quad (1.3)$$

but
$$F_p \leq 1.5F_u \quad (1.4)$$

The current (1980) maximum allowable bearing stress, $1.5F_u$, is approximately 80 percent greater than the previous specification requirement, $1.35F_y$.

The current bearing stress limitations were based on lap splice specimens where the bolt force is applied in the direction of minimum edge distance. When applied to other types of connections, such as the common double angle beam web connection, the new requirements became ambiguous due to minimum edge distances not in direct line of the bearing force. A series of full-scale tests of single row bolted simple beam connections were conducted at the University of Toronto⁵ to check the new requirements. The W18x45 beam shown in Fig. 1.2 was connected to transmit shear to the web, the connection capacity was controlled by bearing using both new and old specifications. The results cited failure mechanisms that had not been anticipated. At failure the bottom bolt split the end of the beam. The factor of safety was 3.0 based on the 1969 AISC Specification⁶ and only 1.8 based on the 1976 RCRS Specification. At the critical bolt location general yielding occurred with high bearing stress. A test on a similar connection but with the compression flange coped, Fig. 1.3, had a 24 percent decrease in strength which was attributed to the cope. The failure consisted of massive hole elongation at

*Only in
? the sense
of gross
distortion.
Hole elongate*

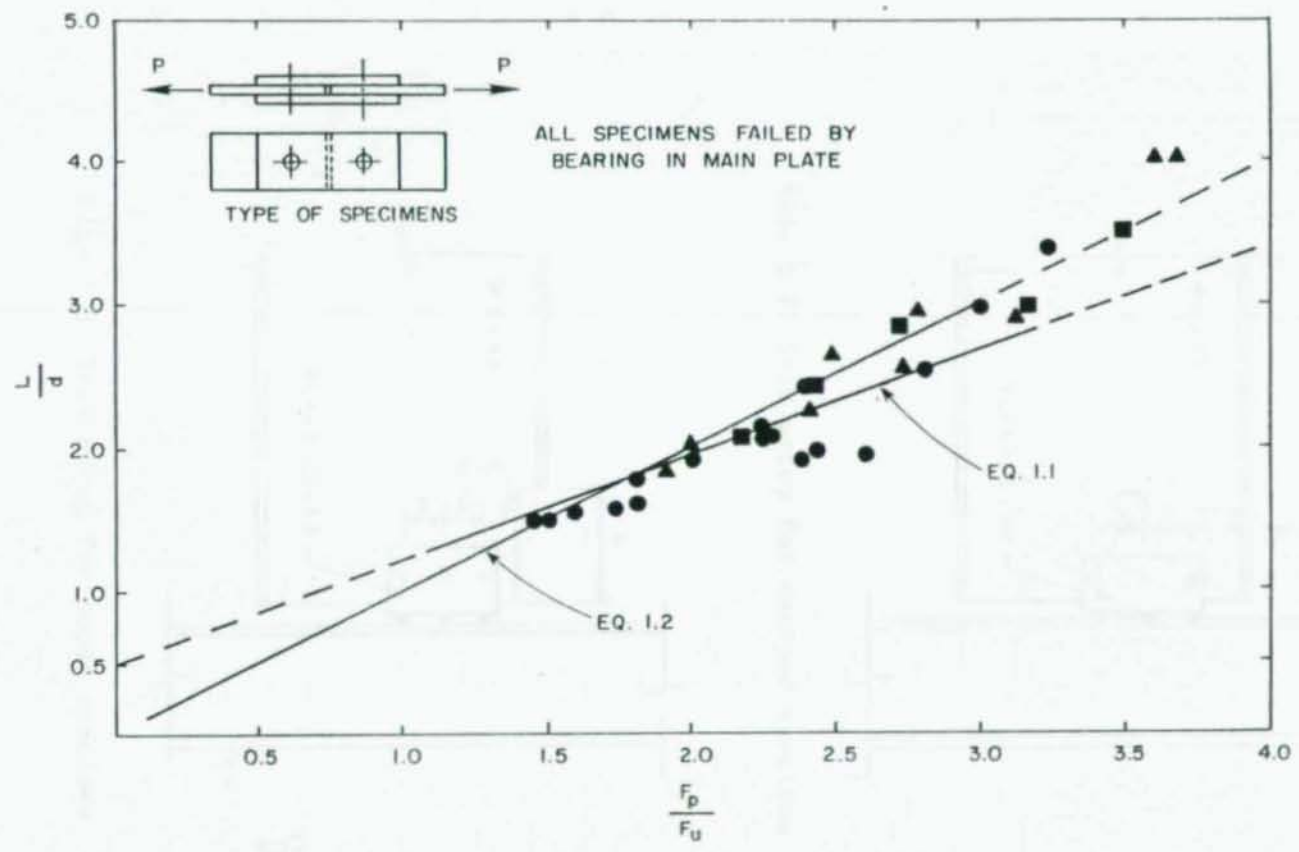


Fig. 1.1 Bearing stress equations plotted against data from lap splice tests (Ref. 4)

the bottom bolt, fracture along lines A-A and B-B in Fig 1.4 starting from the bottom bolt hole, and a local buckling of the web at the cope. This test and similar supplemental tests indicated a failure model where ultimate tensile and shear stresses along sections A-A and B-B, respectively developed simultaneously.

The 1978 edition of the AISC Specification¹ incorporated modifications for the design of coped and uncoped bolted web connections using the new bearing criteria given by Eqs. (1.3) and (1.4). The bearing stress was limited by the edge distance (e_g , Fig. 1.4) Eq. (1.5) and end distance (e_n , Fig. 1.4) Eq. (1.6); the bearing stressed based on end distance neglects any eccentricity on the connection.

$$e_g \geq \frac{2P}{F_u t_w} \quad (1.5)$$

$$e_n \geq \frac{2P}{F_u t_w} \quad (1.6)$$

The 1978 AISC Specification also adopted requirements to limit the stresses on sections A-A and B-B (Fig. 1.4) to prevent a block shear type failure as observed in the Toronto tests. A limit of $0.3F_u$ was set for shear stress and $0.5F_u$ for tensile stress which is shown in Fig. 1.5 and expressed mathematically by Eq. (1.7).

$$R \leq A_v 0.3F_u + A_t 0.5F_u \quad (1.7)$$

Equation (1.7) was incorporated into the 1978 AISC Specification in order to account for the potential failure mechanism which may occur when a bolted web connection is designed to transmit a shear force R to a coped beam over a relatively small portion of the web depth. A connection of this type where the connection depth is less

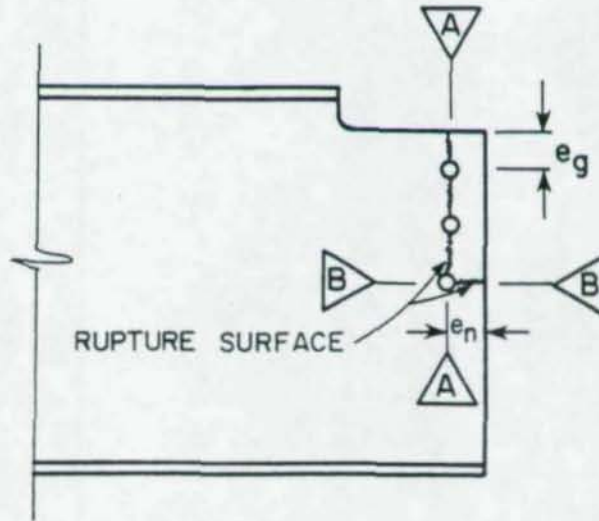


Fig. 1.4 Failure of connection caused by fracturing along plane A-A and B-B.

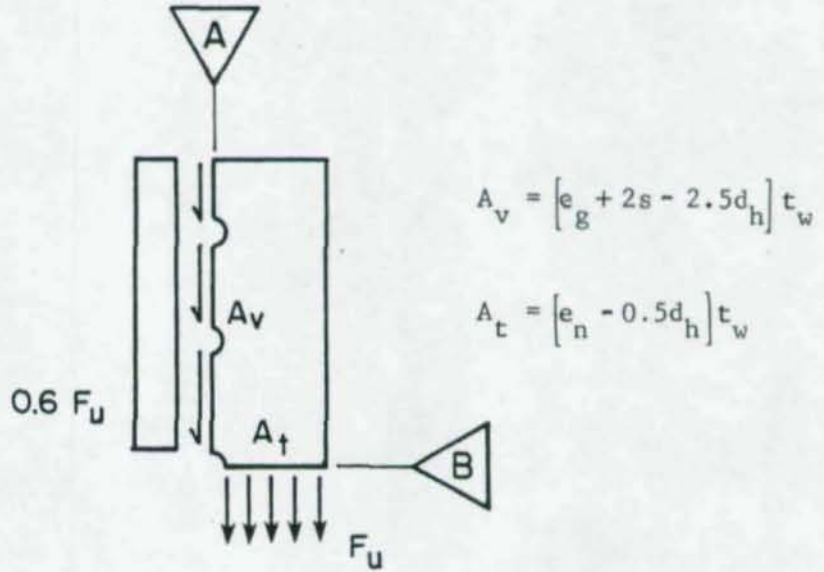


Fig. 1.5 Block shear failure model.

than one-half the beam depth will be referred to as a compact connection.

The two beam tests reported by Birkemoe and Gilmor⁷ exposed the block shear mode of failure, but the limited experimental program did not address potential interacting factors such as minimum end and edge distance, multiple rows of holes, and the type of hole (standard or slotted). A research program sponsored by the American Institute of Steel Construction (AISC) was developed to investigate these problems. The objectives of these tests reported herein focus on the behavior of compact double row shear connections. Only a few tests have been conducted on connections with double rows. Kulak⁸ and Higgins⁹ examined the effects of eccentricity, and Munse¹⁰ studied the moment-rotation behavior of standard riveted and bolted connections.

A total of eight compact double row bolted shear connections on W18x60 beams were tested. The behavior was examined and the connection capacities compared with the 1978 AISC Specification. An elastic finite element program was used to analyze the connections in order to develop a simple failure model. Design recommendations for simple bolted shear beam connections are presented.

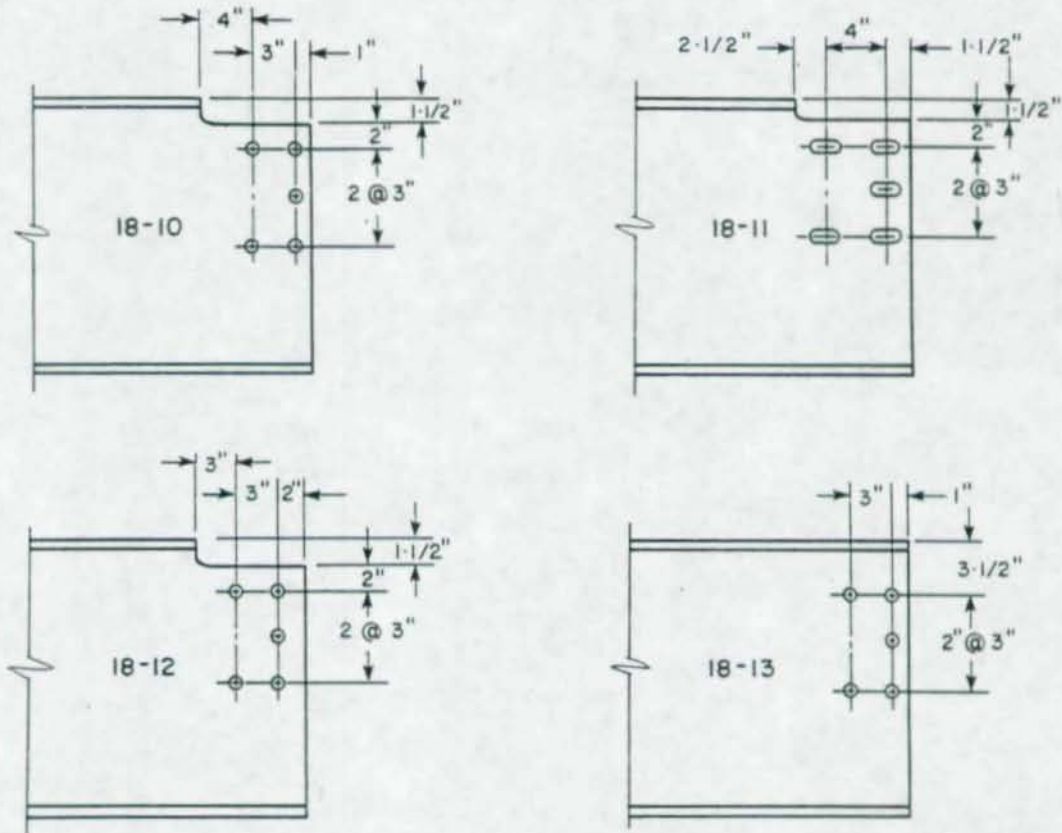
CHAPTER 2

TEST PROGRAM

Test Specimens

Eight tests were conducted on compact, double row bolted shear connections with framing clip angles on both sides of the web, as shown in Fig. 2.1. The principal parameters considered in preparing test specimens were edge distance, slotted holes, the number of bolts and their arrangement, and coped compression flanges. The test beams were W18x60 with flame cut edges. The minimum edge or end distance of one inch shown are the minimum values permitted by the 1978 AISC Specification. The test beams were from two heats of A36 steel, tests 18-10 through 18-13 from heat 1 and tests 18-16 to 18-19 from heat 2. The tensile coupon test results for the two heats are listed in Table 2.1; standard ASTM coupons and procedures were used.^{11,12} The coupons were cut from areas subjected to elastic stresses of two beams after the connection tests were completed. Web coupons were taken in both the longitudinal and transverse direction since the primary cause of failure of the connection tests was fracturing in the web.

The framing clip angles used in the test connection were all L7x4x3/8 except for test 18-11 which had a pair of L8x4x1/2 clip angles. The thickness of the clip angles was chosen in order that the test connection remain flexible yet the failure of the connection would occur in the web. Thirteen-sixteenth (13/16) in. diameter holes for the 3/4-A325 bolts were used for the test connections with standard holes; 1-15/16 x 13/16 in. slotted holes were used for test 18-11. The A325 bolts had no threads in the shear plane and were tightened by calibrated wrench. The bolts



Note: All holes $13/16$ in. ϕ
 diameter, slotted holes
 $1-15/16$ in. \times $13/16$ in.

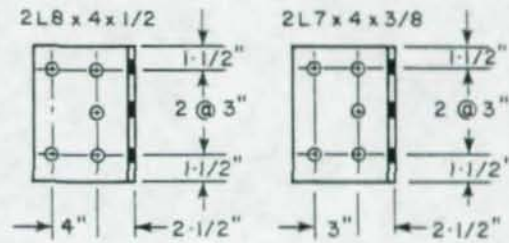


Fig. 2.1a Detail of connection specimens from heat 1

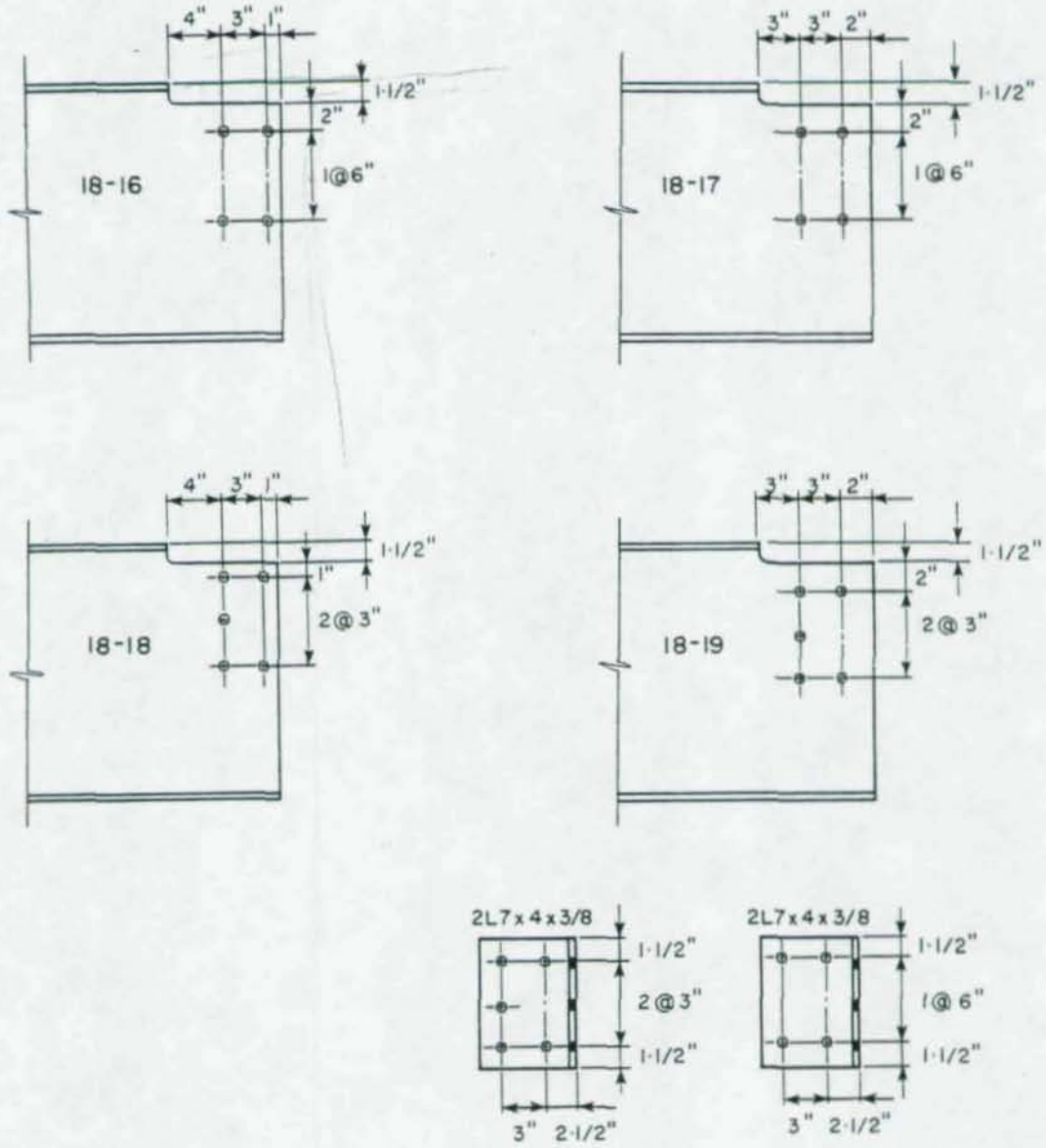


Fig. 2.1b Detail of connection specimens from heat 2

TABLE 2.1 TENSILE COUPON TEST RESULTS REPRESENTING HEAT 1 AND HEAT 2

Heat 1						
Coupon Property	Tension Flange	Compression Flange	Longitudinal Web A	Longitudinal Web B	Transverse Web C	Transverse Web D
Static yield (ksi)	36.7	36.2	38.2	38.9	38.4	37.9
Static ultimate (ksi)	57.5	58.1	61.3	59.2	59.3	59.1
Elongation (%)	28.5	29.7	28.9	28.7	19.1	23.0
					Average Web Strength (Static)	
					F _y - 38.3 ksi	
					F _u - 59.7 ksi	
Heat 2						
Coupon Property	Tension Flange	Compression Flange	Longitudinal Web A	Longitudinal Web B	Transverse Web C	Transverse Web D
Static yield (ksi)	33.5	34.3	39.5	34.4	35.6	36.7
Static ultimate (ksi)	56.7	57.3	58.2	56.1	58.5	59.2
Elongation (%)	32.6	32.6	24.8	32.9	25.0	34.4
					Average Web Strength (Static)	
					F _y - 36.6 ksi	
					F _u - 58.0 ksi	

were placed in bearing against the holes in the test connection before being tightened. The bolts were tightened to meet the minimum bolt tension of 28 ksi required for 3/4 in. diameter A325 bolts by the 1978 AISC Specification. To obtain the desired tension in the bolts the necessary torque applied by the wrench was determined by the procedure suggested by Stewart.¹³

Test Setup

The test arrangement shown in Fig. 2.2 permitted the individual testing of a connection on each end of the 10 ft. long test beam. The end of the beam with the connection being tested was framed into a W10x89 column stub. A roller support and calibrated load cell were placed approximately 18 in. from the other end so it would be undisturbed when framed to the column for a later test. Load was applied to the test beam 24 in. from the face of the column stub by a 200 ton hydraulic ram. The load position was chosen to produce failure in the connection and not the test beam. A channel section was bolted to both sides of the web at the ram location to prevent web crippling. Roller assemblies were placed under the reaction load cell and above the loading ram so that longitudinal movement would not be restricted.

The test frame consisted of a reaction beam, column and thrust bracket. The thrust bracket and column were anchored to the floor by 3 in. diameter threaded studs to prevent vertical movement and in-plane horizontal movement of the frame. The framing system supported the reaction at the load cell and the column stub. The reaction beam was fabricated by bolting two wide flange steel beams together with high strength bolts at 6 in. intervals along the span. The same type of friction connection attached the column stub to the thrust bracket. To help prevent slippage of these friction connections, the surfaces in the shear plane were sanded to obtain greater roughness. Out-of-plane

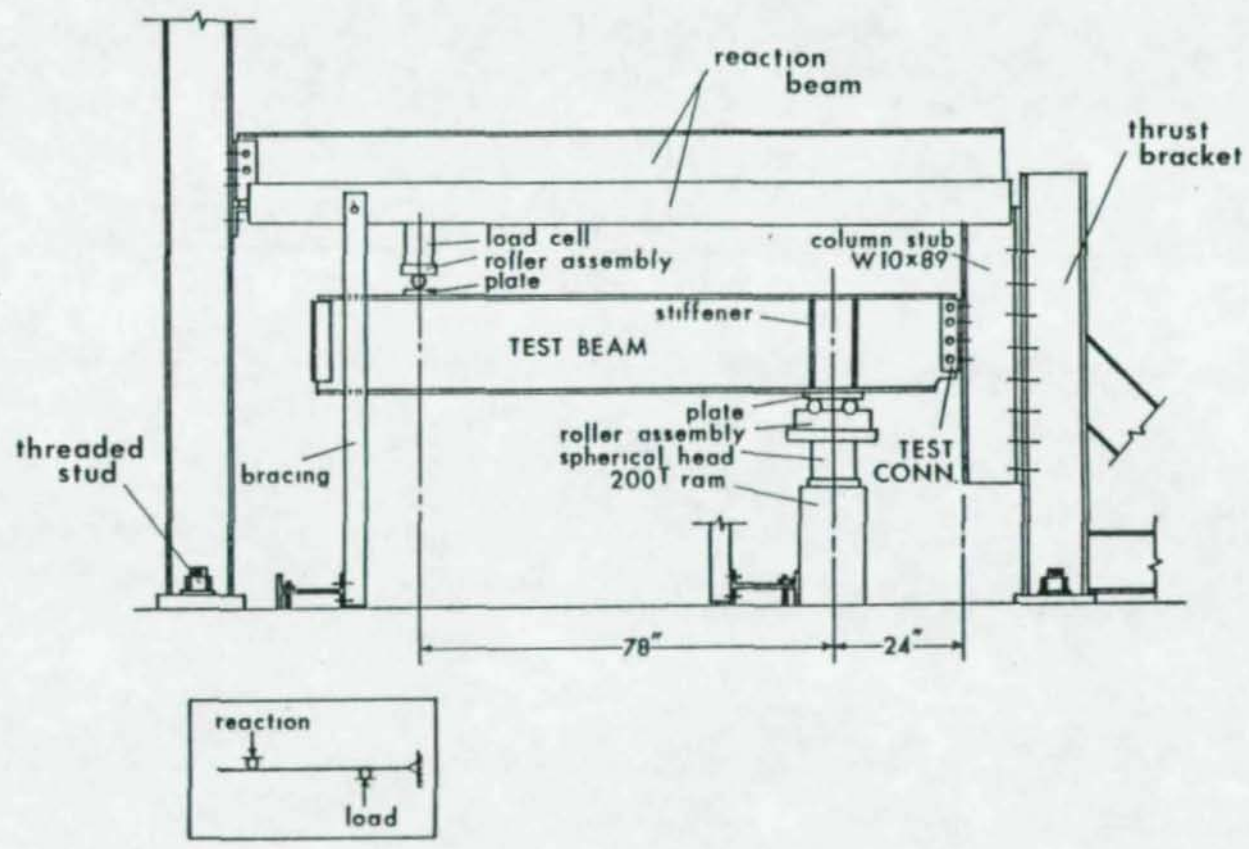


Fig. 2.2 Test setup schematic

movements of the support frame were prevented by a bracing system shown in Fig. 2.3. Plates with slotted holes that were attached to the bracing system prevented lateral movement of the test beam's flanges, shown in Fig. 2.4, but allowed vertical movement of the beam. Additional plates laterally braced the test beam's compression flange near the test connection. Any in-plane horizontal movement was prevented by the thrust bracket.

Instrumentation

The hydraulic ram was controlled with a handpump. The magnitude of the applied load was established by a pressure transducer and verified by a second transducer connected to a x-y plotter and by a pressure gage. The far end reaction was determined with a calibrated load cell. With this arrangement the moment and shear at the test connection could be determined by statics. Vertical deflections were measured using dial gages which had 0.001 in. intervals. Vertical movement was recorded at the load point and in the vicinity of the test connection at the locations shown in Fig. 2.5. Gages 1 and 2 helped to determine when elongations and fracture occurred in the web in the direction of applied shear. A potentiometer attached near dial gage 2 and wired to the x-y plotter also measured the vertical movement of the top flange at the test connection. Relative horizontal movement between the clip angle and the web was measured by sighting with a transit on scales with 0.02 in. graduations, as shown in Fig. 2.5. Scales were placed against the clip angle at two locations and also on the beam web. Knowing the relative horizontal movement of two points on the clip angle and the distance between the two points, the rotation of the clip angles could be determined by assuming rigid body rotation between the two points. The beam's rotation likewise could be determined. As a second means of establishing beam rotation an inclinometer was placed on the top flange to measure end rotation of the beam.

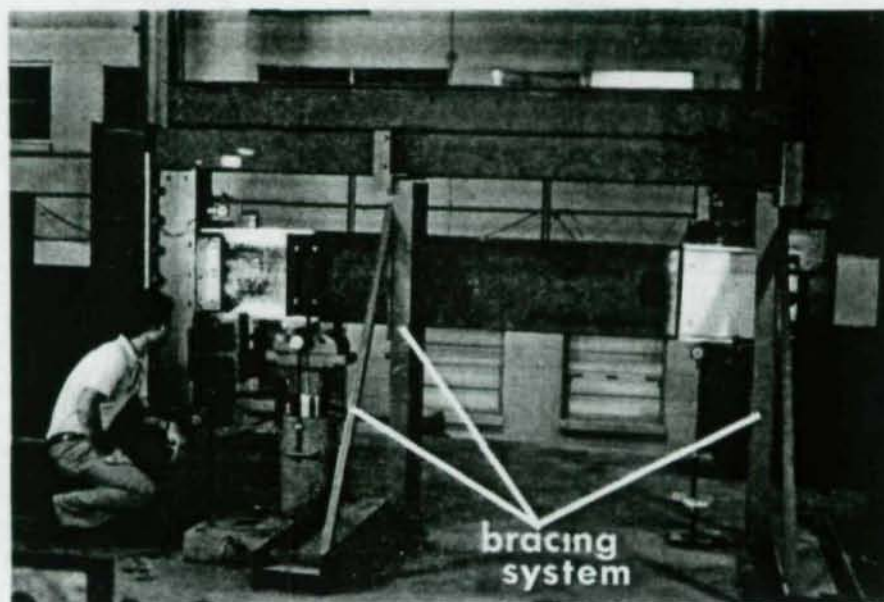


Fig. 2.3 View of bracing system supporting the test frame and test beam

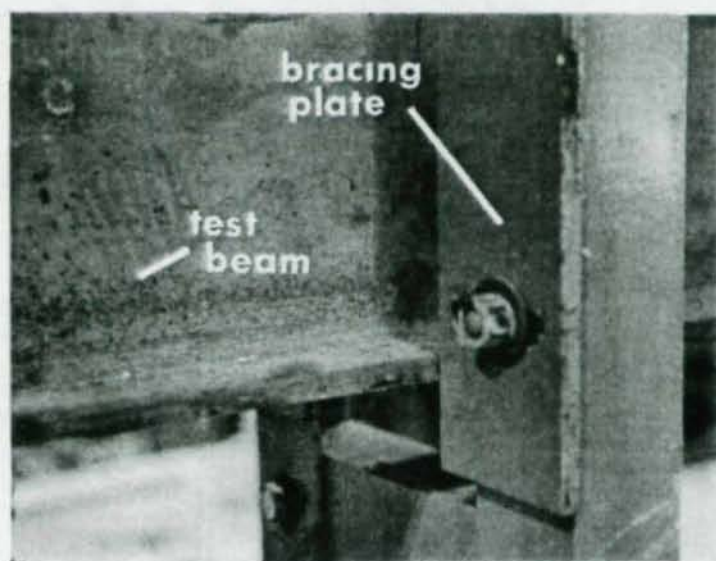


Fig. 2.4 Closeup of bracing plates

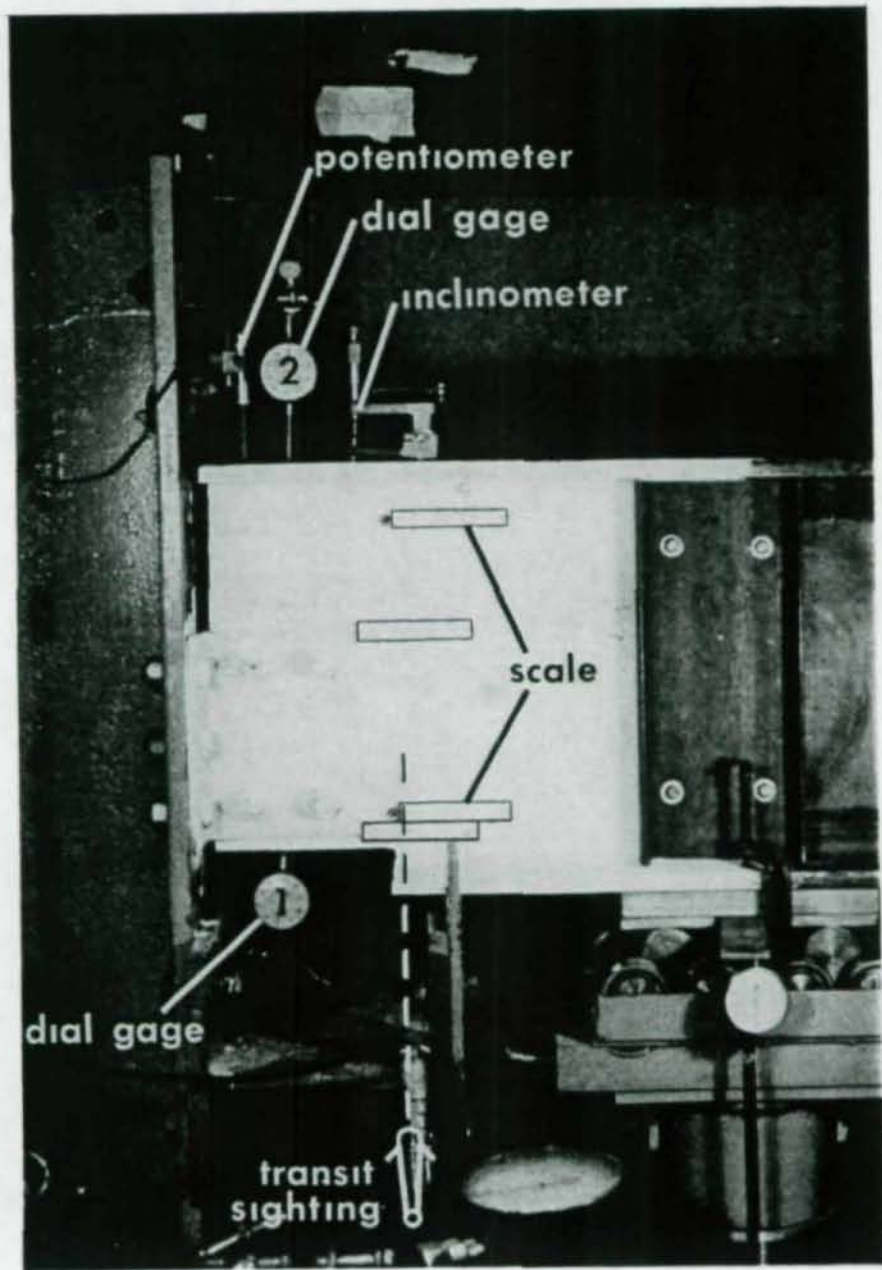


Fig. 2.5 Instrumentation at the connection

Test Procedure

Prior to each test, the web area, flanges and clip angles in the vicinity of the connection were whitewashed to provide a visual display of yield patterns. Only the web on one side of the beam was whitewashed; the other side of the beam's web had a 1 in. square grid scribed onto a silver painted background to document the deformations. In testing the connections, the load was applied in increments and the data recorded approximately five minutes after each load increment so that the load and deformation could stabilize when yielding occurred. The test was terminated when the maximum load was reached and unloading commenced or when the connection deformations were excessive. After completion of a load test the beam was rotated, the connection on the opposite end was bolted to the column stub, and a new test conducted.

CHAPTER 3

EXPERIMENTAL BEHAVIOR

An evaluation of the test data showed that in general a plot of end reaction R at the connection versus the vertical deflection at the clip angle Δ_1 or Δ_2 gave the best quantitative description of connection behavior throughout the test. Because the behavior of the connections was similar, only one typical test, 18-12, will be discussed in detail. The discussion of test 18-12 is followed by a presentation of photos of all the failed connections along with some comments. The plots of connection reaction versus deflection containing descriptive captions are in Appendix I for all the tests; the nominal connection dimensions appear in the figures, the actual dimensions are listed in Table 1-II of Appendix II. A summary of the experimental ultimate capacity of the connections is in Chapter 5 under Table 5.1.

Figure 3.1 shows the plot of connection shear versus the deflection above and below the connection, as recorded from dial gages 1 and 2. The same result is plotted in Fig. 3.2 using only the deflection measured by dial gage 2. During the test, yielding first appeared in the web near the connection below the bottom line of the holes (line B in Fig. 3.1) followed by fracturing in the web along the bottom horizontal line of fasteners. The separation of the two curves after load point 4 in Fig. 3.1 indicates when the fracturing starts in the connection. The net deflection between dial gages 1 and 2 is a measure of deformations within the connection and separation of the material in the web due to fracture. Figure 3.3 shows a plot of net deflection. After fracturing occurred yield lines appeared in the web between the horizontal plane where fracture

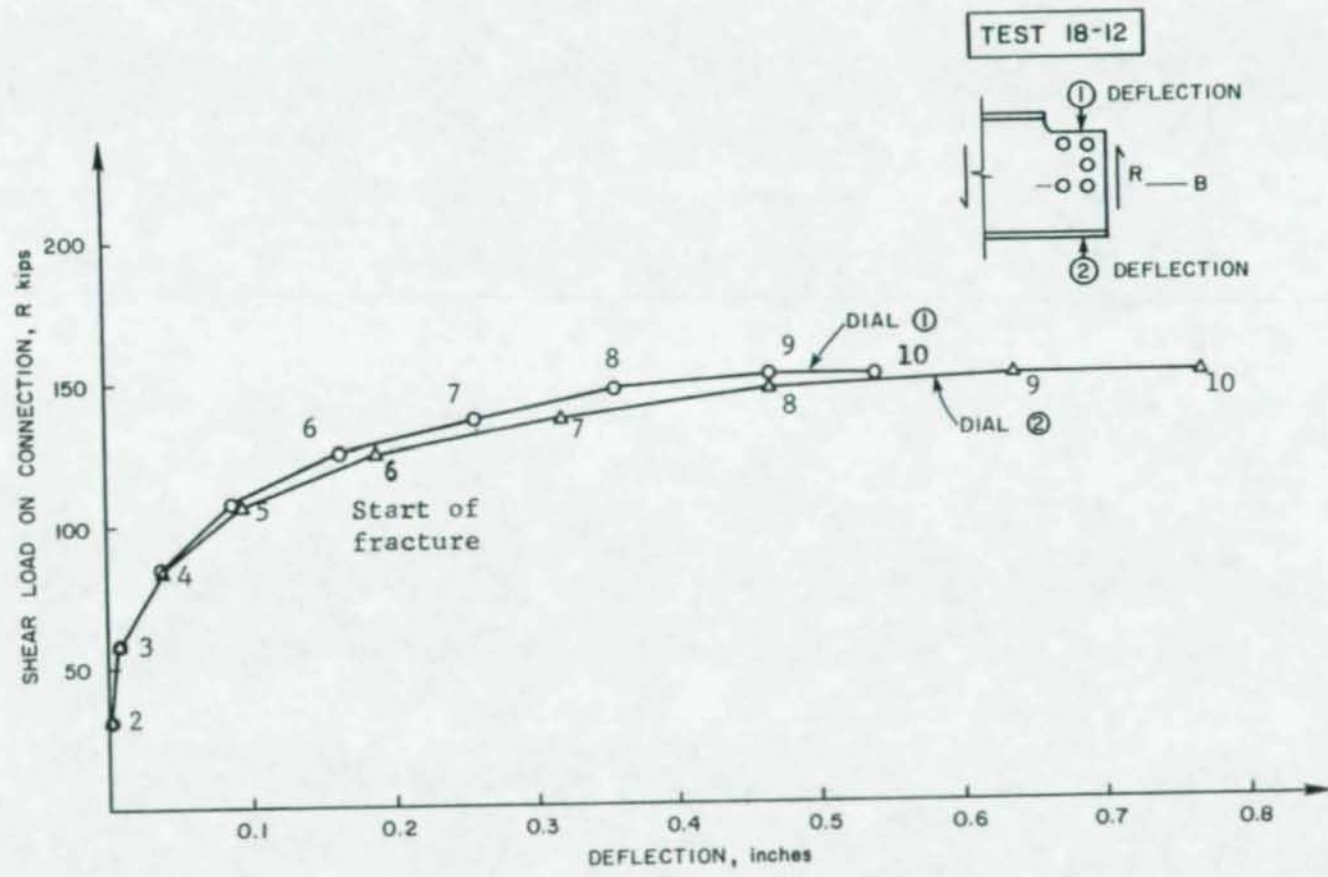


Fig. 3.1 Connection reaction versus connection deflection

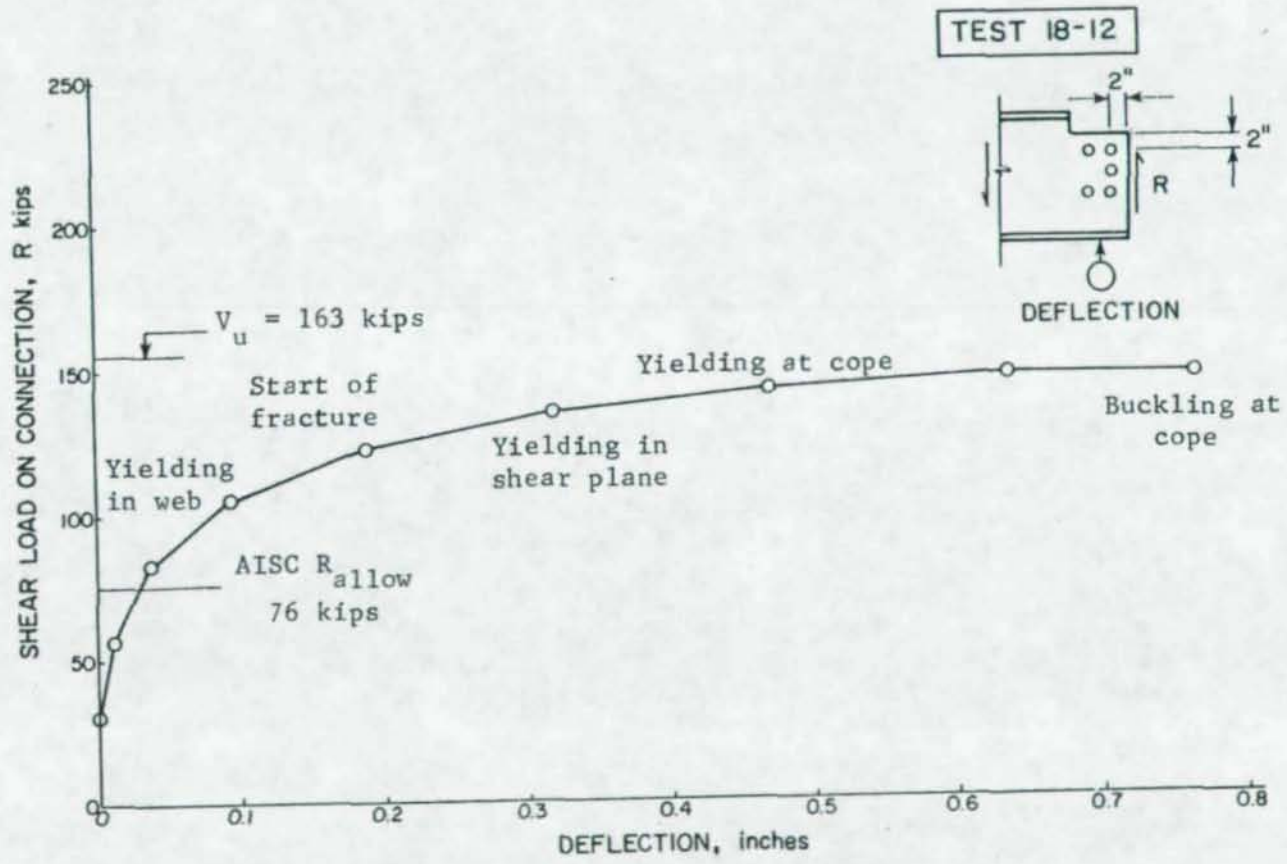


Fig. 3.2 Connection reaction versus deflection of tension flange

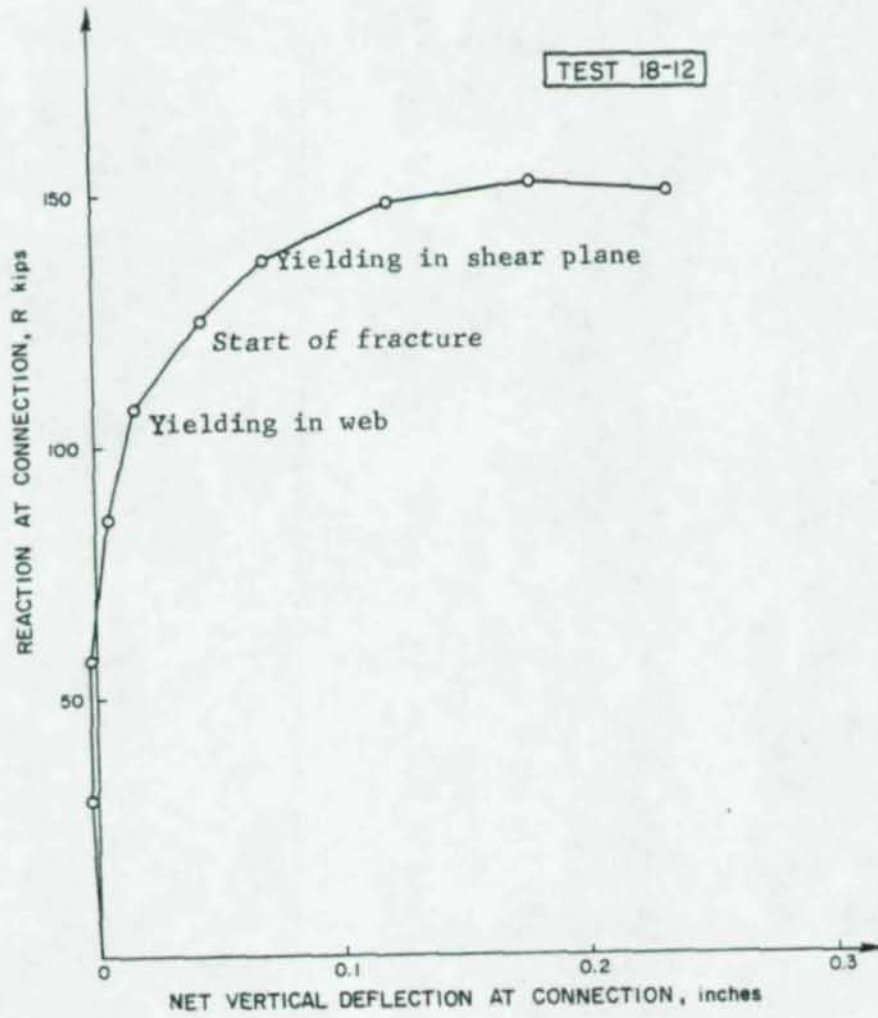


Fig. 3.3 Connection reaction versus net deflection of connection

occurred and on the top of the beam at the connection. Figure 3.4 shows the behavior described; the fracturing in the web is not noticeable in the figure. The yielding that occurs after fracturing could be caused by shear, and also by flexural stresses as illustrated in Fig. 3.5. The buckling of the web at the cope that appeared at R_{max} could be a result of this flexural yielding; however, the buckles appeared after the web had undergone excessive deformation and the beam web had fractured.

Test 18-12 had an allowable reaction R_{allow} of 76 kips based on the 1978 AISC Specification which was controlled by the top edge distance with an applied eccentricity factor. Further discussion of the 1978 AISC Specification related to the test connections and a summary of allowable loads is given in Chapter 5. The shear yield capacity, V_u , of 163 kips for test 18-12 assumes a uniform shear stress equal to $F_y/\sqrt{3}$ over the gross area of the web at the cope, $A_w = d_n t_w$. These values are shown in Fig. 3.2.

Figure 3.6 shows the plot of applied load versus deflection at the point of load. The deflection of the load point increased rapidly once the connection showed signs of yielding.

The connections tested were flexible shear connections which in design are assumed to act as simple supports and allow the beam to rotate without developing any moment at the connection. However, all connections will develop some end moment. A flexible connection will restrict some rotation of the beam's end. Figure 3.7 shows the rotation of the clip angles versus the moment developed at the connection. Some of the erratic behavior at the early stages may be due to experimental error. The moment at the connection is determined by subtracting the load times 24 in. from the product of the load cell and its distance from the face of the column stub. Since the products are large and the difference is close to zero, a small discrepancy in the load cell or pressure transducer

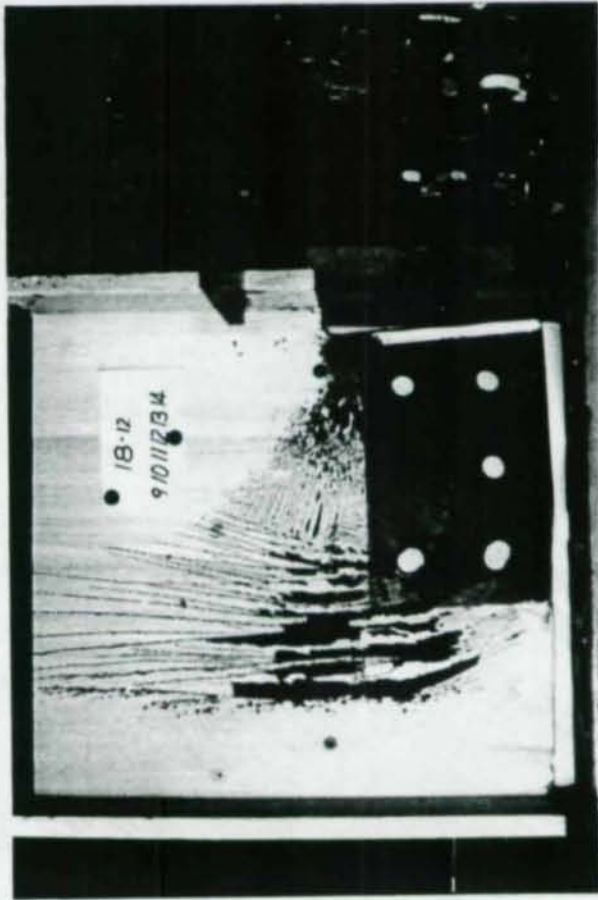


Fig. 3.4 Test 18-12 after failure

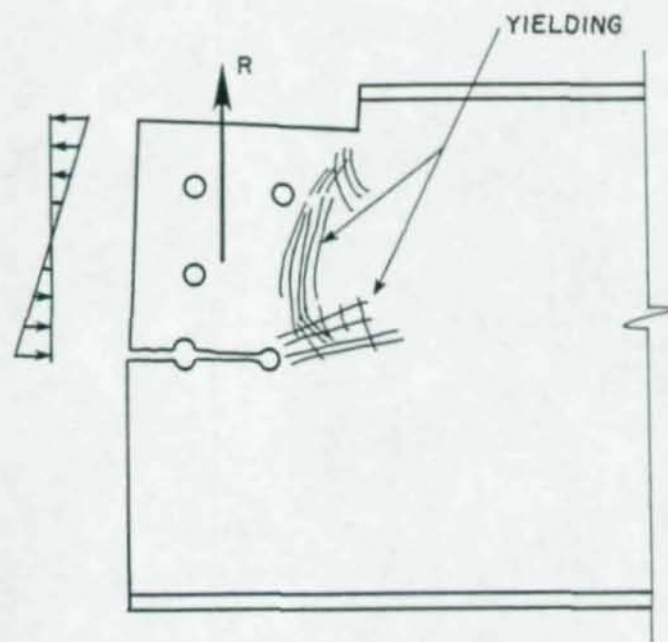


Fig. 3.5 Flexure stresses caused by connection rotation about vertical plane

TEST 18-12

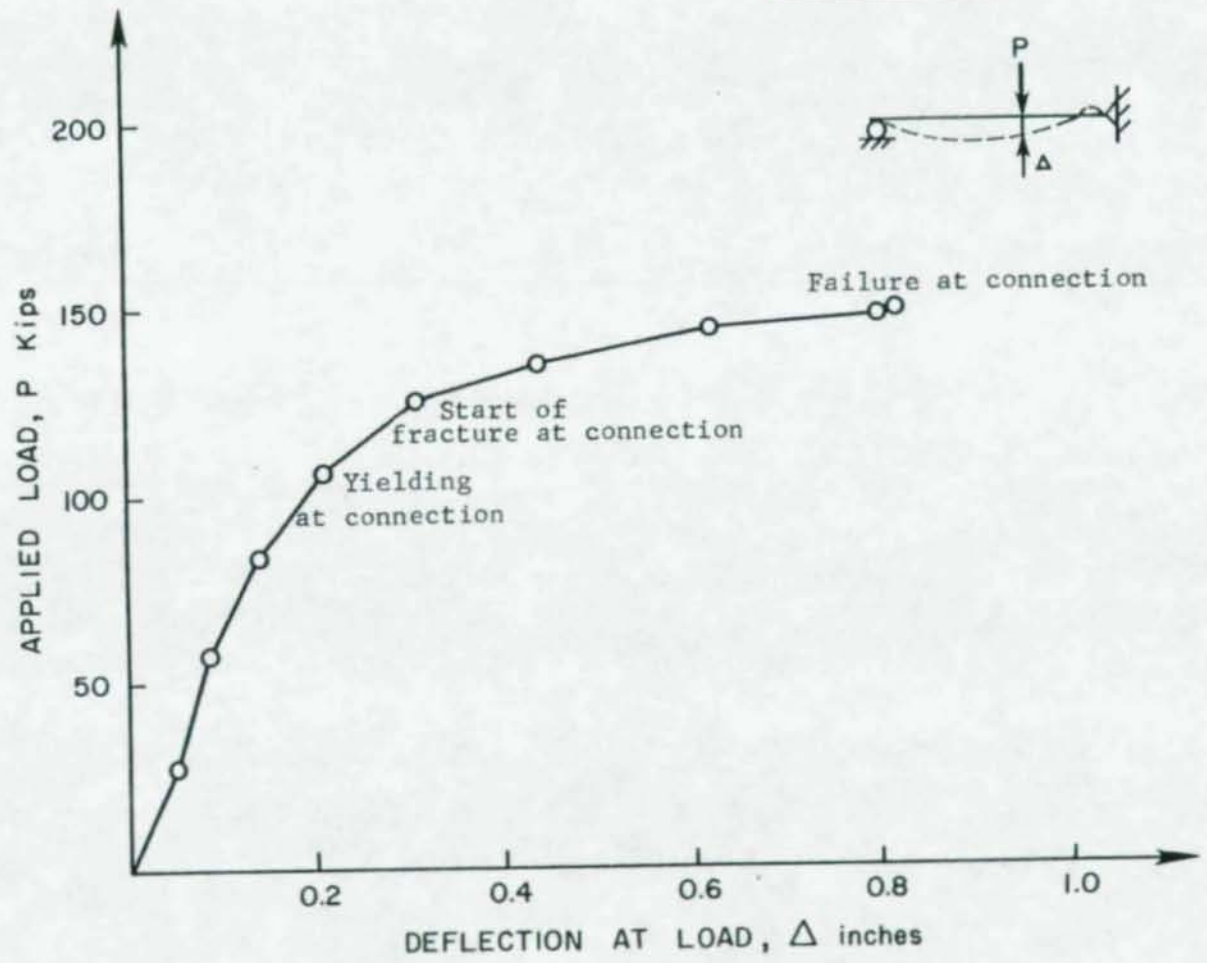


Fig. 3.6 Applied load versus deflection at point of load

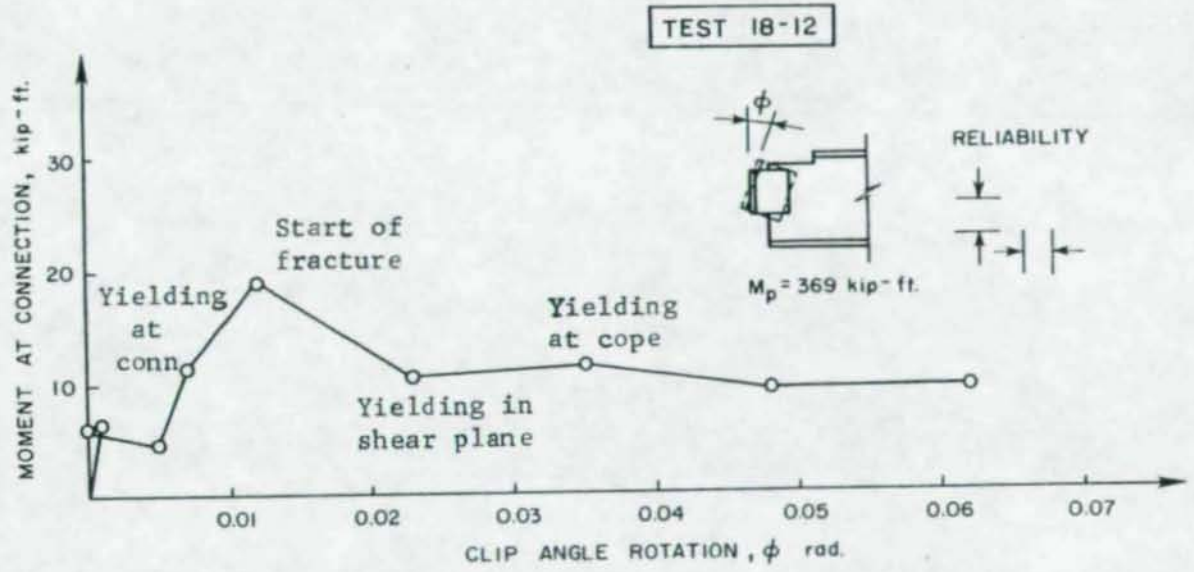


Fig. 3.7 Moment developed at the connection versus rotation of clip angles

reading can lead to a larger discrepancy in the moment. The experimental reliability noted in Fig. 3.7 is based on an 0.65 kip error in load cell reading and an 0.02 in. error in the transit reading used to measure the rotation. Figure 3.8, which shows a plot of connection reaction R versus the point of inflection from the column stub face (eccentricity), is also not too smooth because of the same problem. However, the significance of Figs. 3.7 and 3.8 is that the point of inflection shifts and the moment at the connection depend on what stage of failure the connection is at. The connection becomes more flexible as the load is increased due to the yielding and fracturing in the beam web.

Figure 3.9 shows a plot of connection reaction R versus rotation at the connection; the beam end rotation and the clip angle rotation are superimposed on the same plot. The curves indicate that once the yielding and fracturing occur the beam will rotate with respect to the clip angles. The difference in rotation between the clip angles and the beam is due to the clip angles yielding in the outstanding legs, shown in Fig. 3.10, as they are pulled away from the column, and also due to rotation of the beam web within the connection once fracture occurs in the horizontal plane in the web as depicted in Fig. 3.5. With most of the beam rotation occurring in the web above the plane of fracture, the tension flange below the connection will not rotate. Thus the inclinometer which was placed on the tension flange showed less rotation than the clip angles. The maximum rotation of 0.012 radians that occurred at the beam's end is equivalent to the rotation of a similar beam with a 20 ft. simply supported span subjected to a uniform load which would cause the plastic moment, M_p , to be reached at midspan.

All of the failed connections appear in Fig. 3.11 with the clip angles removed, the ultimate capacity of each connection is

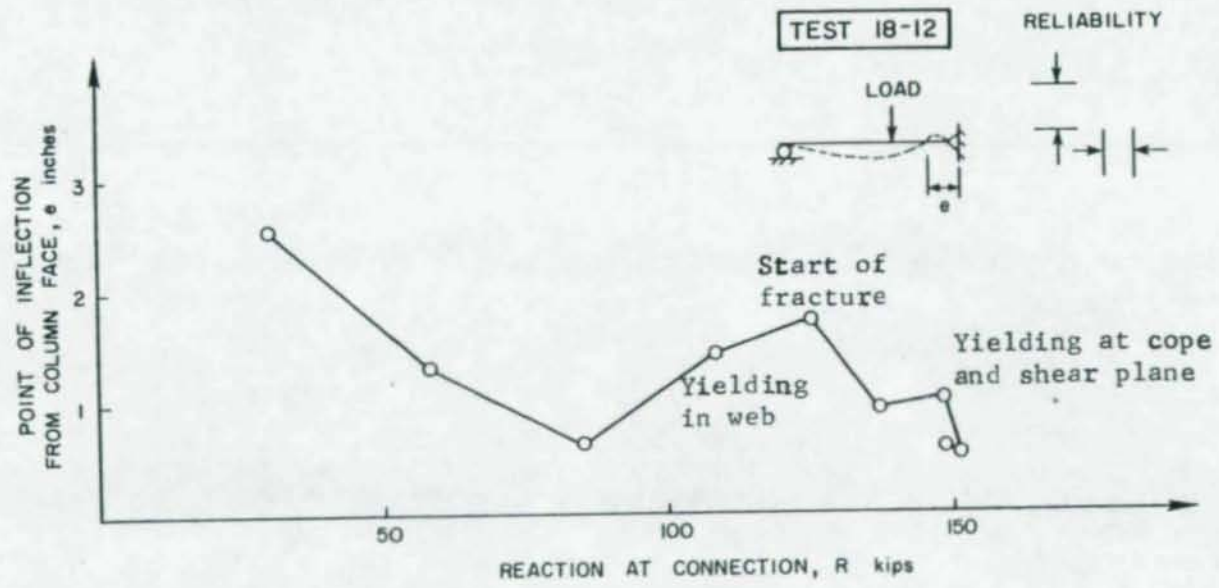


Fig. 3.8 Plot of the location of the point of inflection versus the reaction at the connection

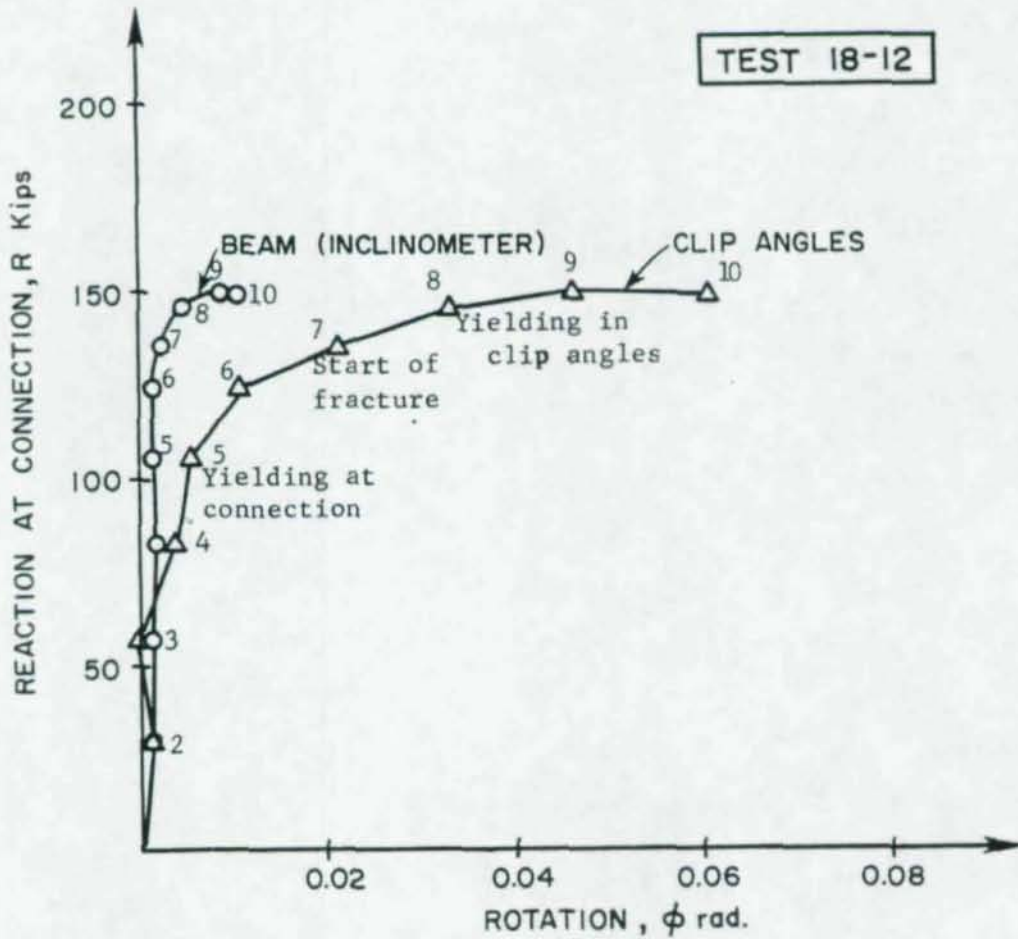


Fig. 3.9 Reaction at the connection versus the rotation of the clip angles and the beam

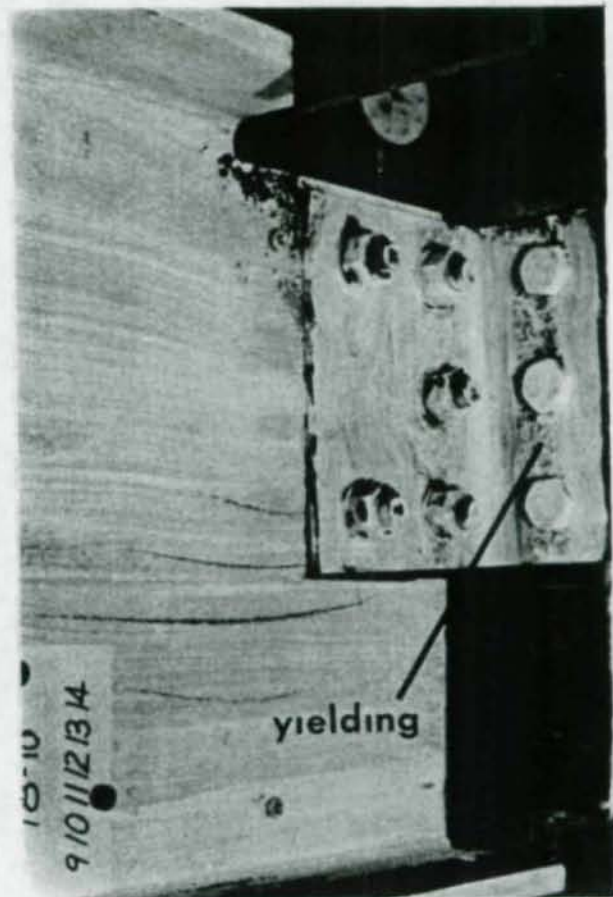
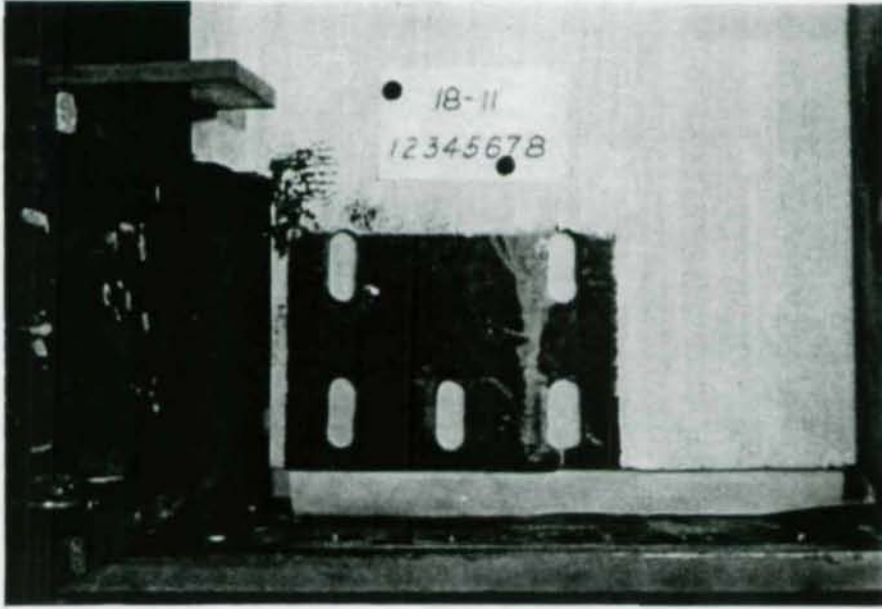
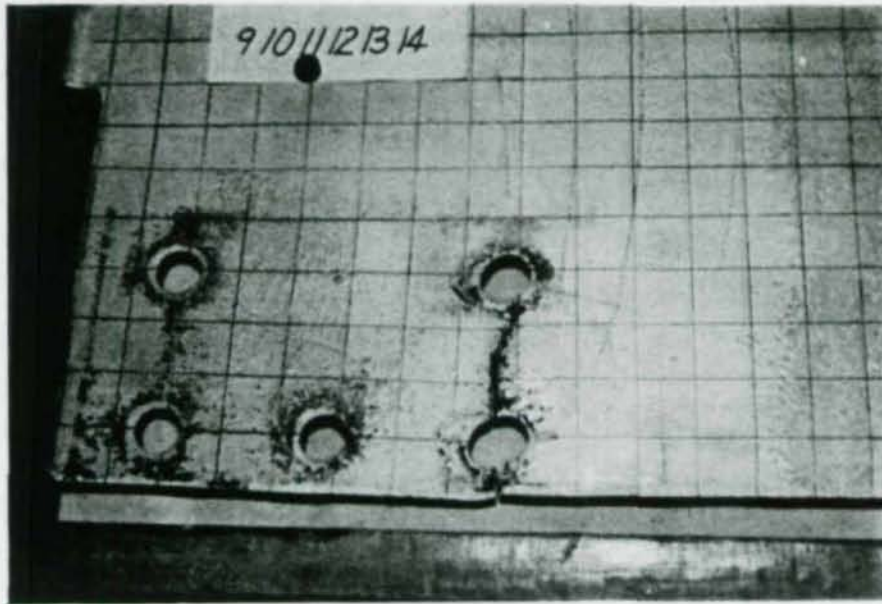


Fig. 3.10 Yielding in the outstanding legs of the clip angles

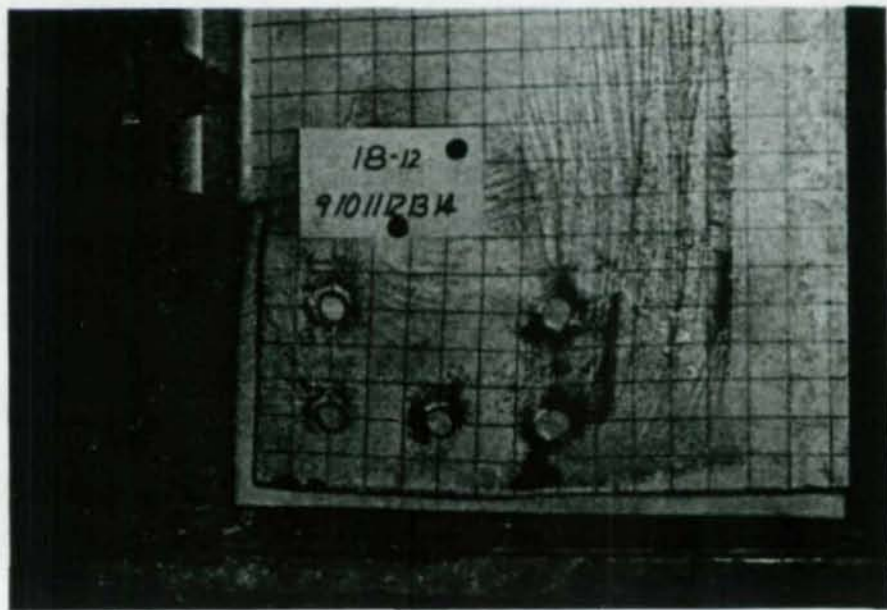


Test 18-11, $R_u = 101$ kips

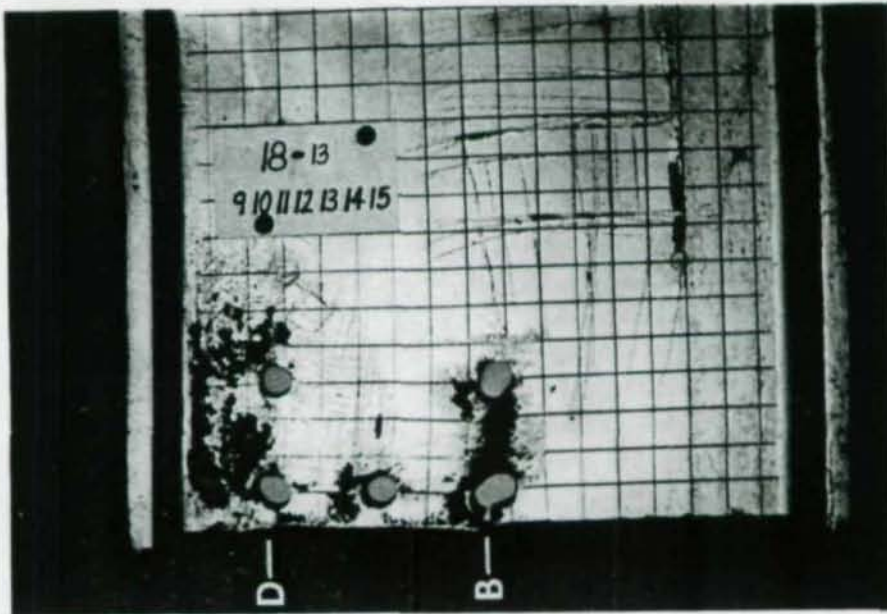


Test 18-10, $R_u = 111$ kips

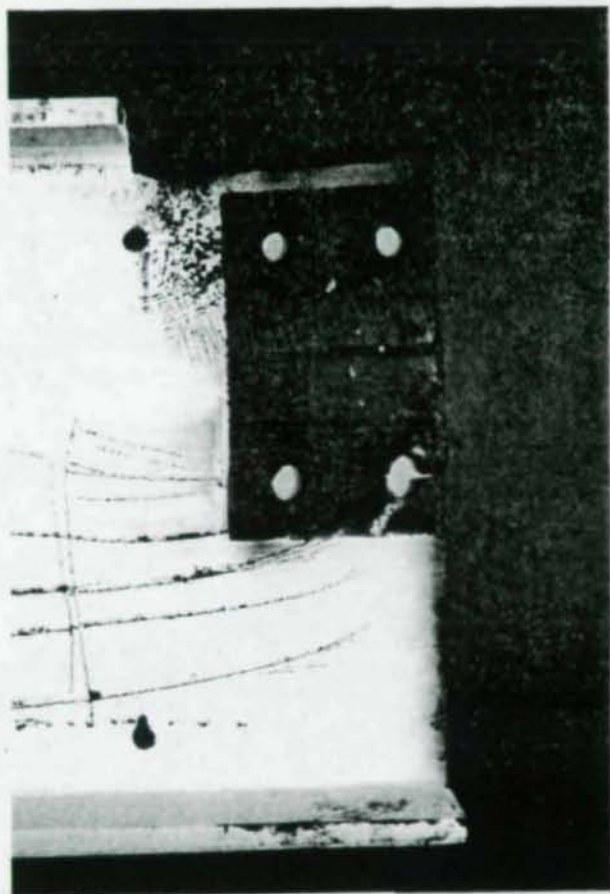
Fig. 3.11 Failed specimens



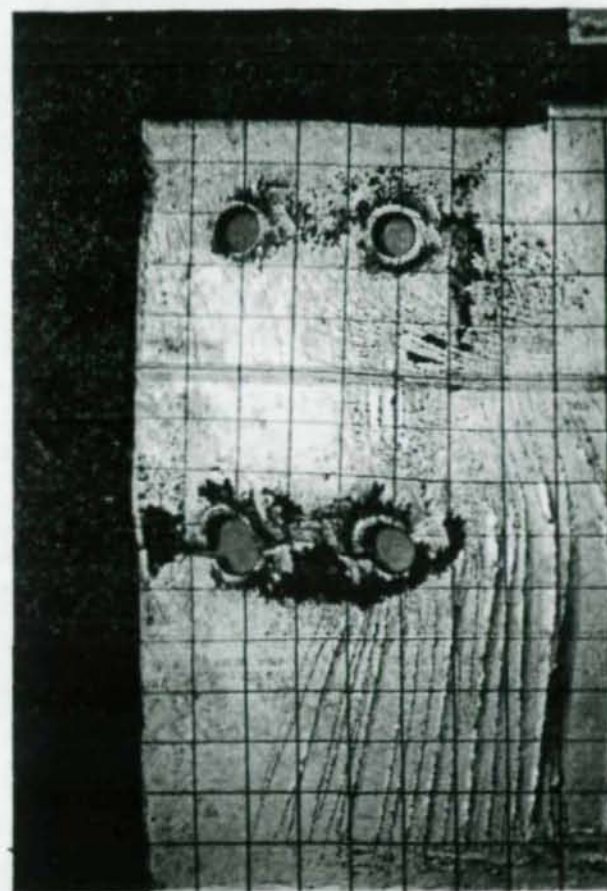
Test 18-12, $R_u = 152$ kips



Test 18-13, $R_u = 140$ kips

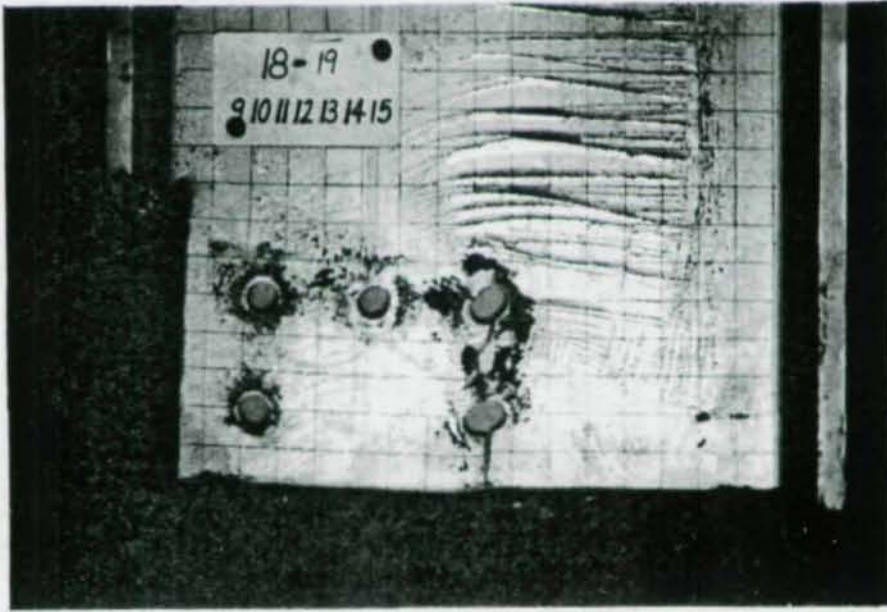


Test 18-16, $R_u = 111$ kips

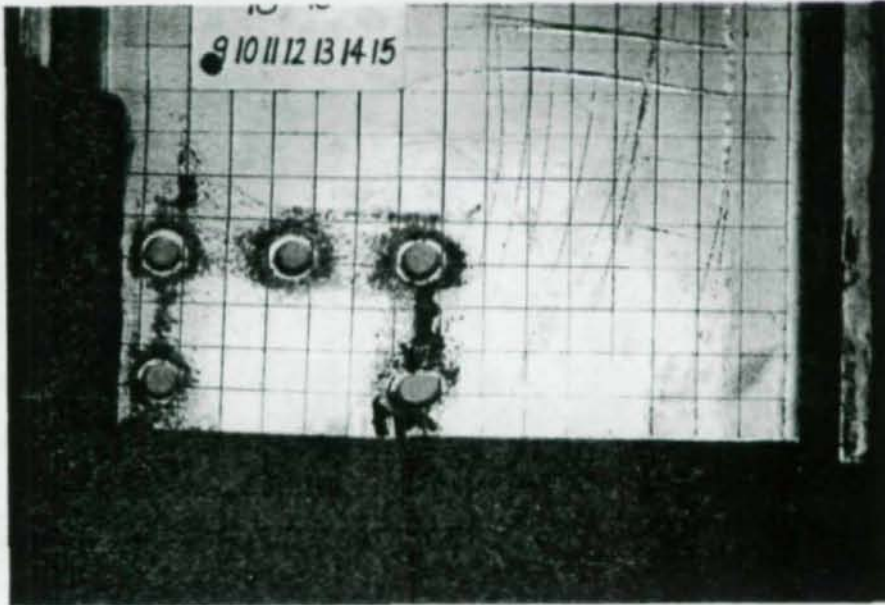


Test 18-17, $R_u = 131$ kips

Fig. 3.11 cont.



Test 18-19, $R_u = 134$ kips



Test 18-18, $R_u = 101$ kips

given as R_u . The specimens showed no significant hole deformation except those located in the horizontal failure plane. Therefore it appears that the shear is not distributed uniformly among the bolts. Test 18-11 which had slotted holes, failed at a load 9 percent less than test 18-10 even though both tests had the identical end and edge distance.

Buckling of the cope which was observed in test 18-12 also occurred in test 18-16, 18-17 and 18-19. Thus the cope buckled in the connections that had only four bolts, or a 2 in. end and edge distance. However, the buckling occurred when the connection had already fractured as described earlier for 18-12.

Test 18-13 involved no cope; once fracturing commenced there was severe compression yielding in the web between the upper row of fasteners (line D in Fig. 3.11) and the compression flange. A small amount of yielding occurred between the bottom line of bolts and the upper line of bolts (line B and line D). However, the web area above the bottom line of bolts along with the compression flange acts as a structural tee in flexural similar to the behavior in Fig. 3.5. Eventually extensive yielding developed in the compression flange 8 in. from the face of the column as shown in Fig. 3.12.



Fig. 3.12 Location of yielding in the compression flange

CHAPTER 4

FINITE ELEMENT ANALYSIS

Purpose

Using the finite element program SAP2¹⁴ a model of the test connection was analyzed in order to obtain elastic stress distributions in the region of the connection. It was felt that such an analysis could provide some guidance to the development of a simple model to predict the connection capacity. The entire W18x60 test beam and L7x4x3/8 clip angles were analytically modeled as shown in Figs. 4.1 and 4.2. The dimensions of the beam's cross section are based on the AISC Handbook.¹⁵

Description of Finite Element Model

The beam and connection were treated as a plane stress, two dimensional model using 4-node quadrilateral elements and 3-node triangular elements with all out-of-plane movement suppressed. In the actual connection the outstanding legs of the clip angles make the connection three-dimensional. Figure 4.3 shows the outstanding legs of the clip angles bending as the beam rotates and pulling away from the column flange. In the finite element model the clip angles were modeled by a connection plate with attached springs. The spring constant of each spring was equivalent to the stiffness of the outstanding leg of one clip angle, enabling the connection to be modeled in two dimensions. Springs were attached only to the top of the connection plate since only this portion of the clip angle pulls away from the column as shown in Fig. 4.3. The value of the spring constant was calculated as shown in Fig. 4.4. The eccentricity of the connection created

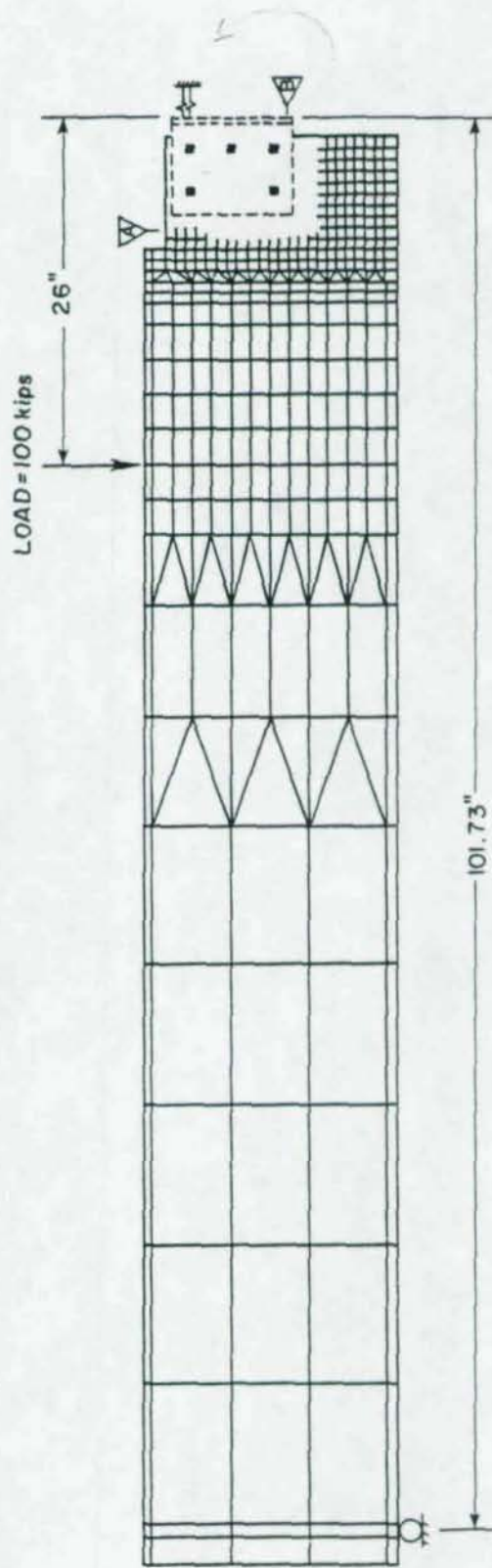


Fig. 4.1 Finite element model of test beam

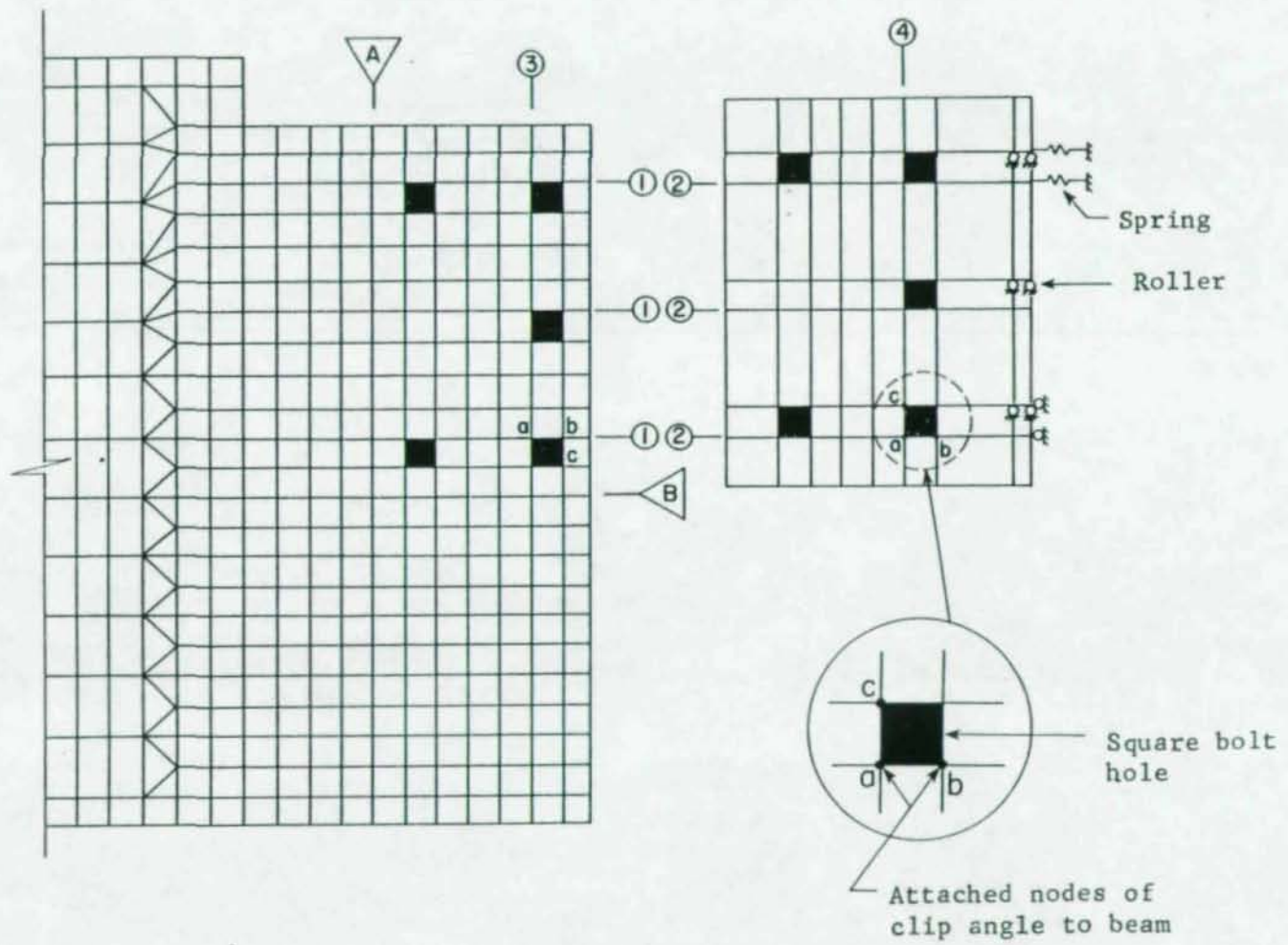


Fig. 4.2 Enlarged view of the finite element model of the connection

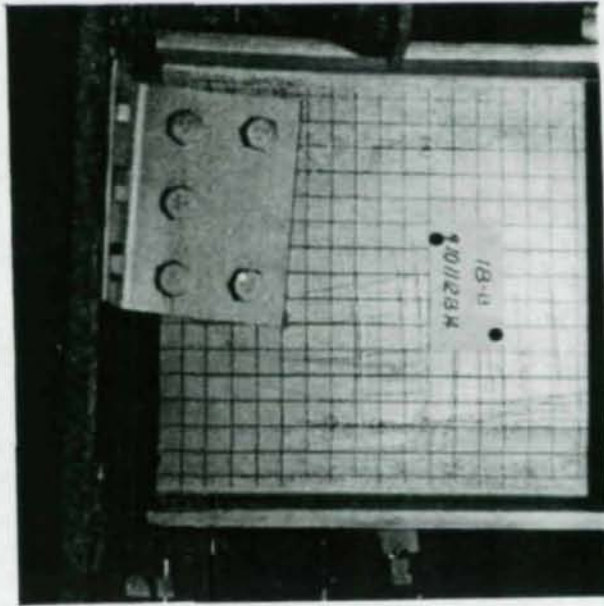


Fig. 4.3a Clip angle behavior

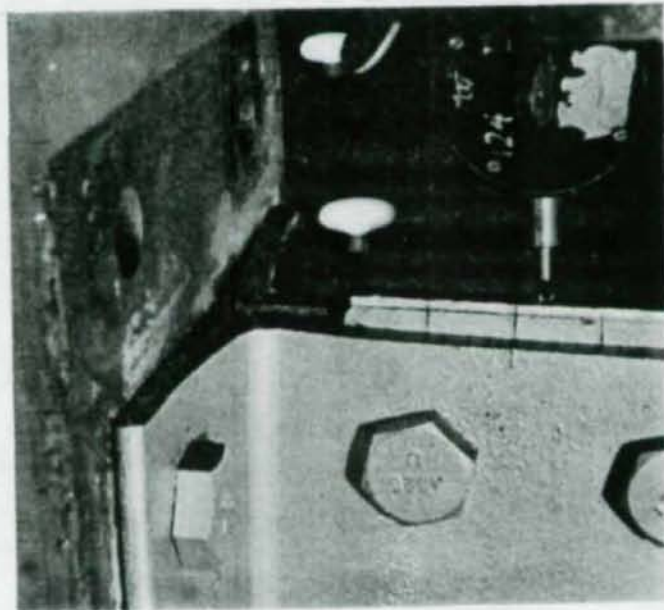
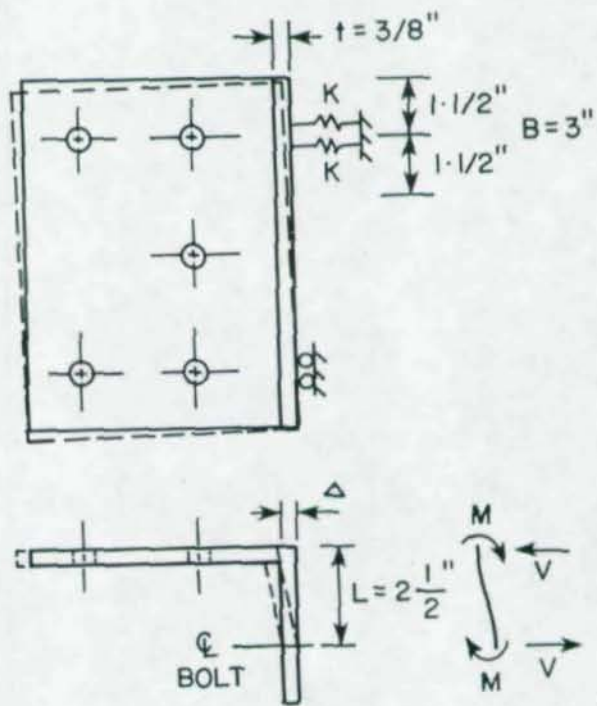


Fig. 4.3b Clip angles pulling away from the column



$$I = \frac{B(t)^3}{12} = 0.0132 \text{ in.}^4$$

$$M = \frac{6EI}{L^2} \Delta$$

$$V = \frac{2M}{L}$$

$$K = \frac{V}{\Delta} = \frac{12EI}{L^3}$$

Spring constant for one clip angle, $K = 293.5$ kips/in.

Fig. 4.4 Modeling of the clip angle

horizontal components of force in the bolts; this force in the upper horizontal line of bolts caused the clip angles to pull away. Hence the dimension B of the clip angle was centered around the upper line of bolts and used as the effective portion of the outstanding legs to resist flexing and pulling away of the clip angles. The bottom part of the clip angles bears directly against the vertical face, thus rollers on a vertical plane were placed at this location on the connection plate. Rollers on a horizontal plane provided vertical equilibrium of the connection plate. Figure 4.2 shows the two-dimensional model with the springs and rollers attached to the connection plate. The finite element analysis produces a moment in the connection of approximately 48 kip-ft. which is within 10 percent of actual test values.

To attach the connection plate to the beam the connection plate was overlaid on the beam's web such that lines 2 were superimposed on lines 1 and line 4 was superimposed on line 3 as shown in Fig. 4.2. The nodes forming one side of the elements on the contact surfaces with the bolt of the bolt holes were made common to elements in the beam and connection plate. The insert of Fig. 4.2 shows the common nodes "a" and "b" on the contact surface with the bolt. These nodes simulated infinitely stiff bolts that connected the clip angles to the beam's web; this simulated actual behavior since no test bolts showed significant deformation. Square holes which appear as darkened squares, were used instead of the standard round holes for ease in modeling. Since in actual testing the bolt only bears on one side of the bolt hole, the square holes in the finite element model could be used if nodes on the contact side of the hole are attached to the connection plate. Preliminary computer models with an additional node "c", shown in Fig. 4.2, were used to consider the observed direction the bolt bears due to eccentricity of the connection; the results showed no significant difference with using only two nodes. Therefore for the connections

modeled only 2 nodes, nodes "a" and nodes "b," were attached per bolt hole between the connection plate and the beam.

Nine analyses were made studying the effect of the bolt end distance, bolt arrangement, and the spacing of the bolts. In all connections modeled, the edge distance to the cope was given a constant value of 1-3/4 in. For each analysis, the same load of 100 kips was applied to the beam at the same location. In modeling the clip angles two situations were considered. Case 1 has a more flexible connection than the other cases; in cases 2 to 9 the stiffness of the connection plate was twice that of case 1. The stiffness of the connection plate for cases 2 to 9 was equivalent to a pair of L7x4x3/8; in case 1 the stiffness of the connection plate was equivalent to one L7x4x3/8.

Finite Element Results

A typical stress contour of the finite element model is shown in Fig. 4.5a with an actual test beam exhibiting yield lines shown in Fig. 4.5b. The analytical stress contour was plotted by drawing contours at 45 degrees to principal stresses of the same value. The plane of maximum shear stress exists at 45 degrees with respect to the principal stress, where according to yield theory slip lines form. Figures 4.5a and 4.5b compare quite well with respect to stress contours; hence the finite element model predicts where the yield lines form in the beam's web near the connection. The calculated vertical stress distribution around the periphery of the connection (plane A and plane B in Fig. 4.2) can be seen in Figs. 4.6 through 4.14. The planes are a distance d , the bolt diameter, away from the edge of the bolt holes to avoid the local discontinuities in the stress distributions due to the bolt holes. The area of interest in the model was the overall connection behavior and not the localized bearing stresses at the bolt holes.

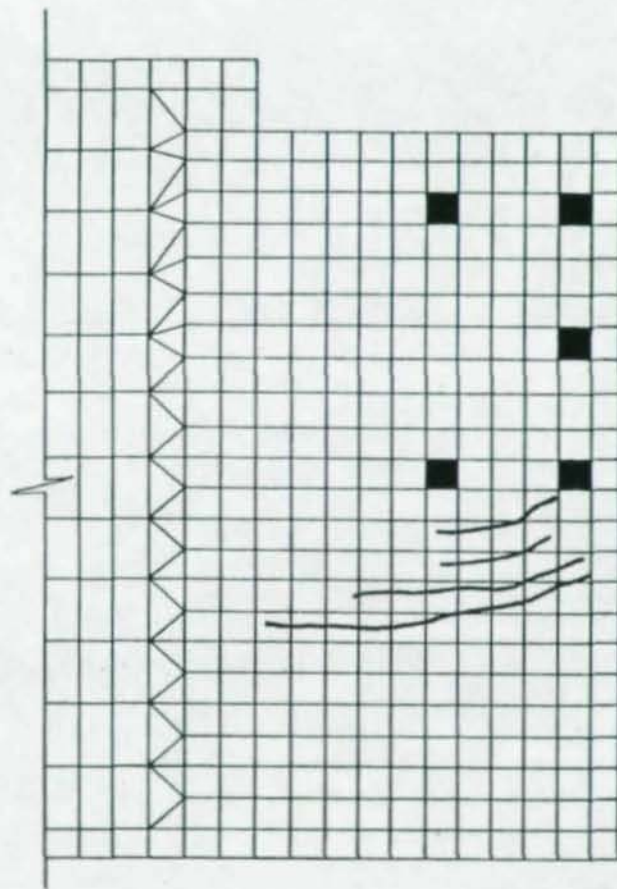


Fig. 4.5a Stress contours from the finite element analysis

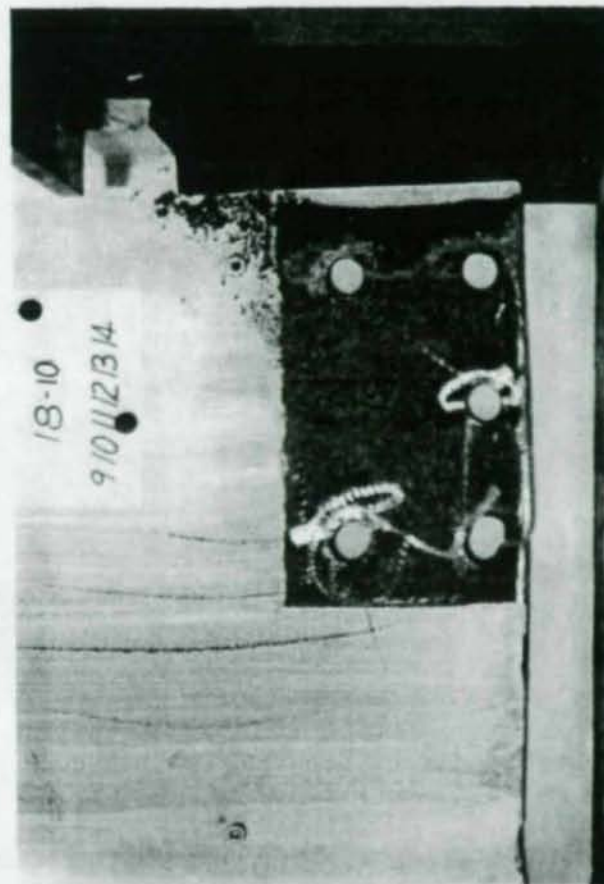


Fig. 4.5b Yield lines in test specimen

CASE 1

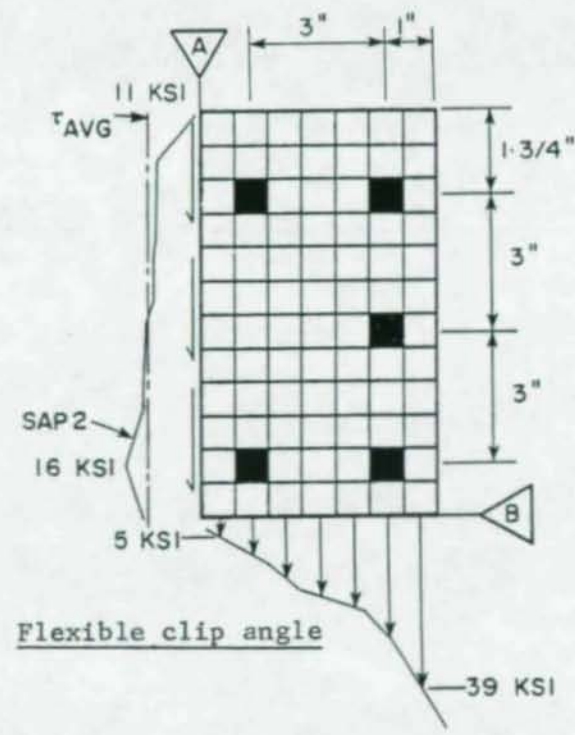


Fig. 4.6 Vertical stress distribution, case 1

CASE 2

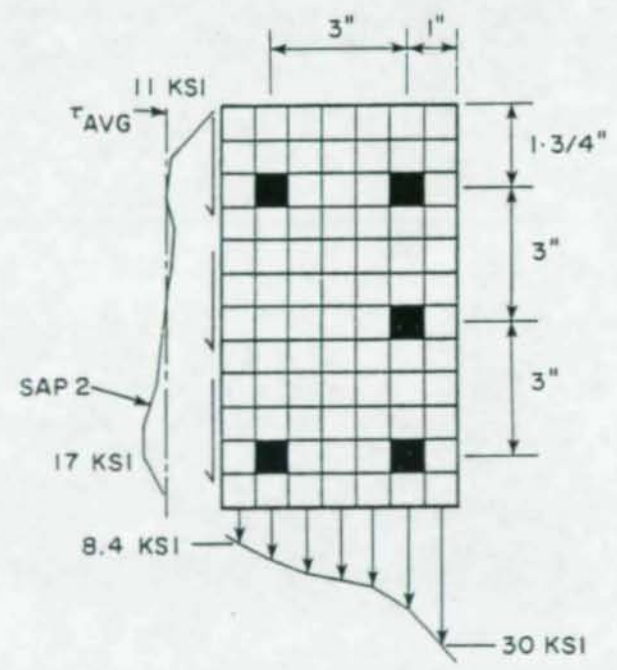


Fig. 4.7 Vertical stress distribution, case 2

*Twisted 3 bars
piles at face
edge*

CASE 3

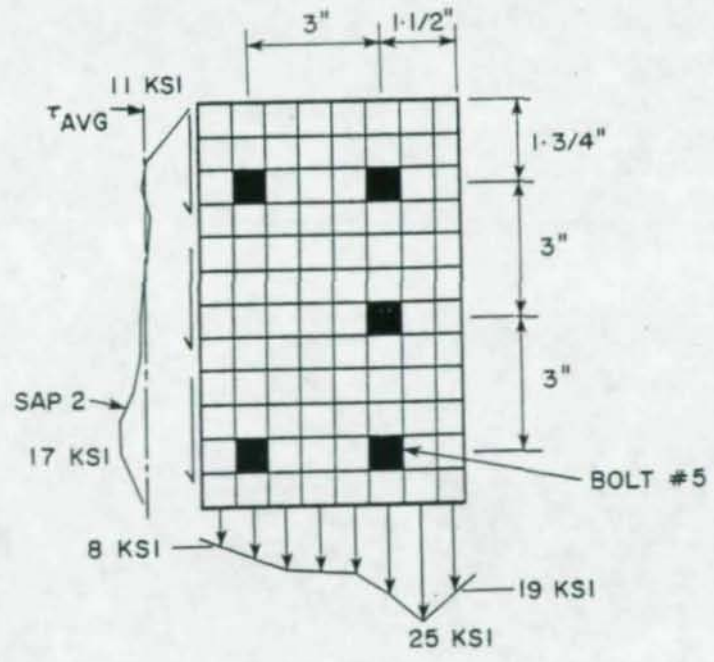


Fig. 4.8 Vertical stress distribution, case 3

CASE 4

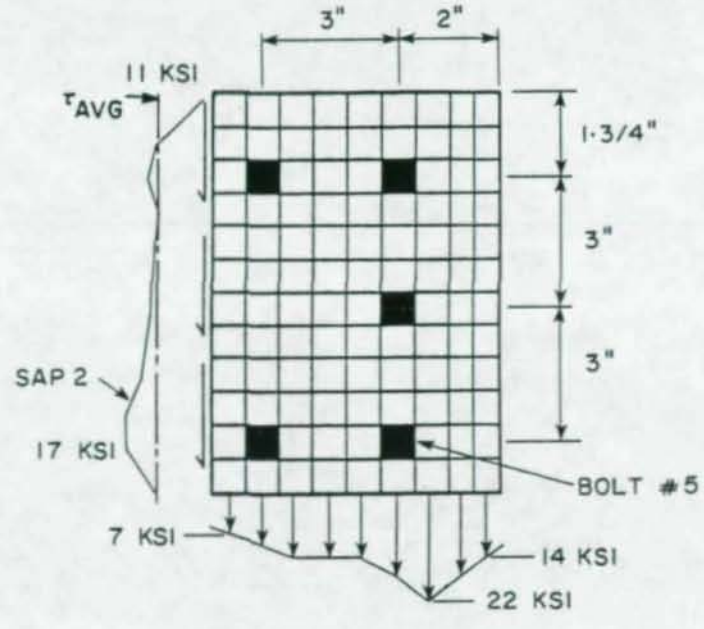


Fig. 4.9 Vertical stress distribution, case 4

Note - Eccentricity to back of connection angles is the same in all connections

Vertical stress softened at edge

CASE 5

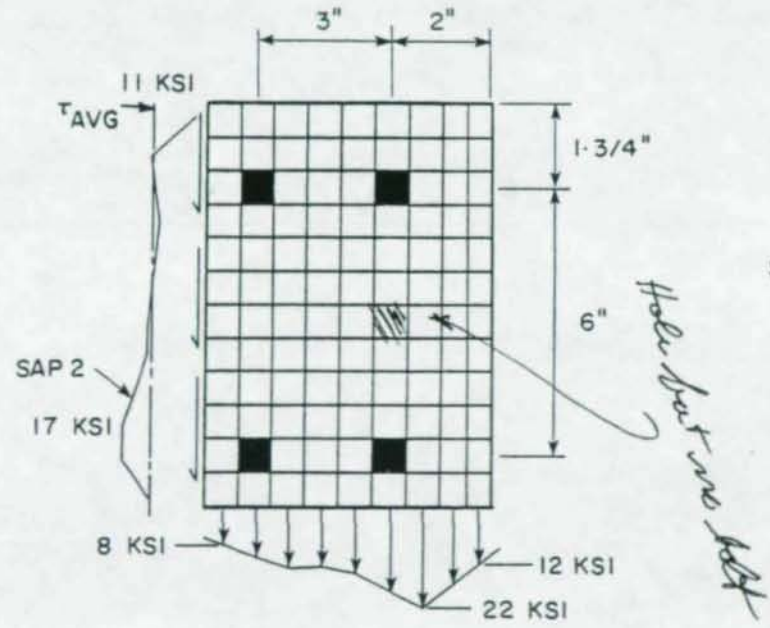


Fig. 4.10 Vertical stress distribution, case 5

CASE 6

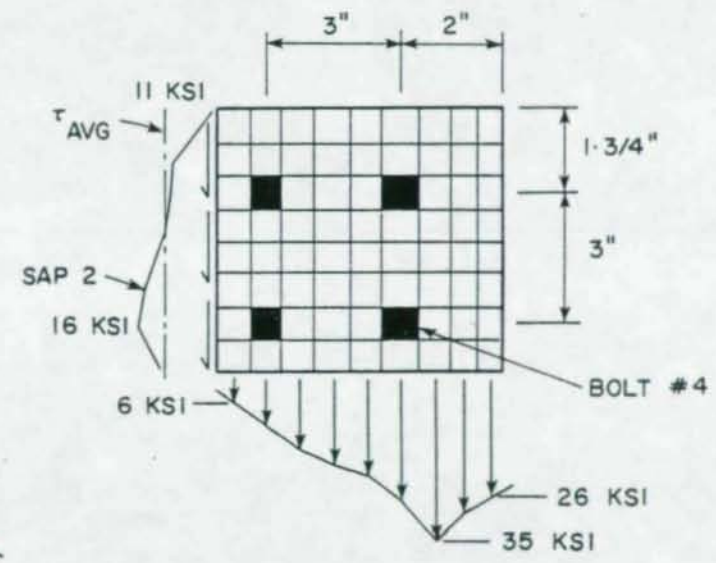


Fig. 4.11 Vertical stress distribution, case 6

CASE 7

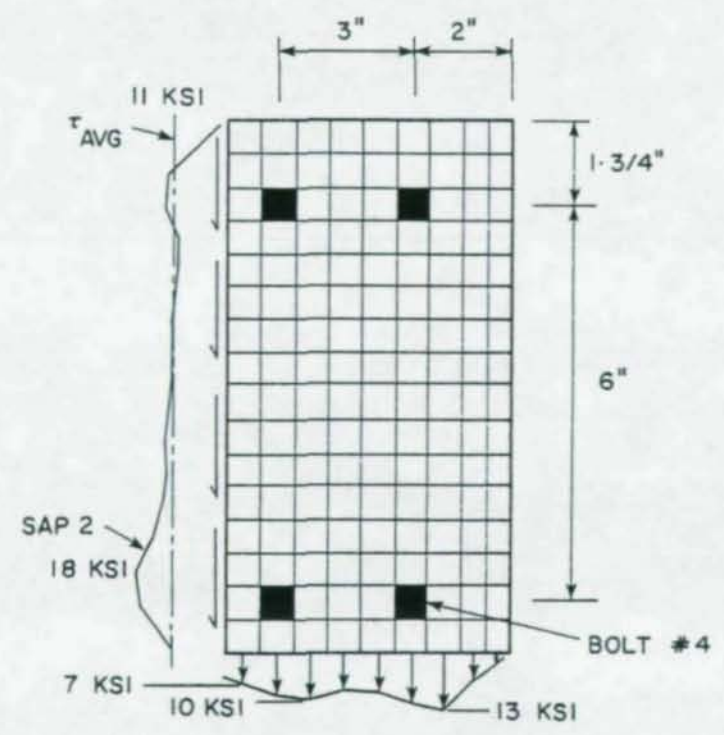


Fig. 4.12 Vertical stress distribution, case 7

CASE 8

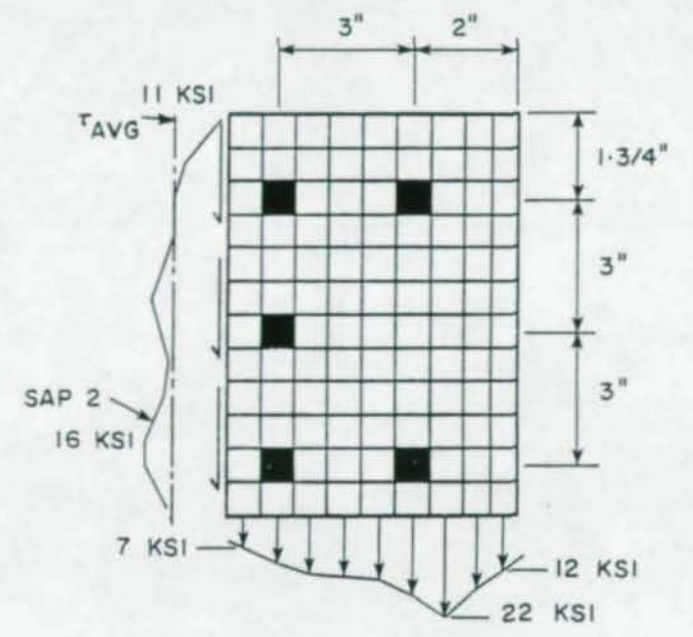


Fig. 4.13 Vertical stress distribution, case 8

CASE 9

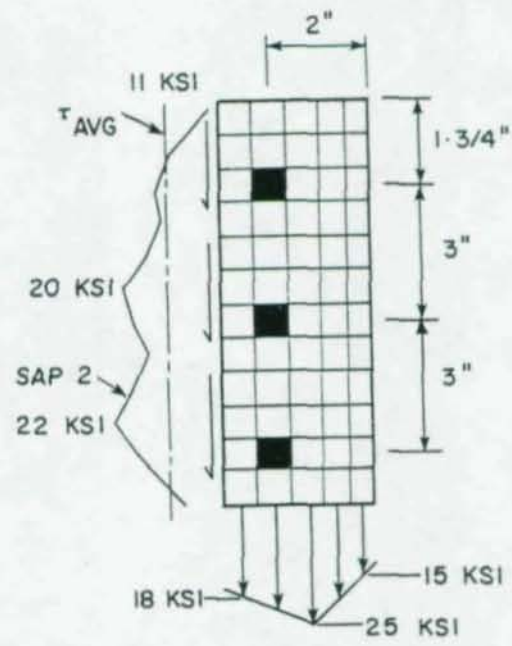


Fig. 4.14 Vertical stress distribution,
case 9

The first connection modeled, case 1, consists of a 5-bolt arrangement with a 1 in. end distance and flexible connection plate. Figure 4.6 shows the shear stress distribution (plane A) and the tensile stress distribution (plane B) for case 1. The horizontal plane has a triangular tensile stress distribution while the vertical plane has a reasonably uniform shear stress distribution. The average nominal shear stress τ_{avg} is shown to be in close agreement with the finite element shear stresses, especially in the region between bolt holes. The average nominal shear stress for all cases is $\tau_{avg} = R / (d_n t_w)$ where d_n is the net beam depth at the cope of 16.611 in.; t_w the web thickness of 0.416 in., and R the reaction at the connection equal to approximately 76 kips for all cases. Hence the average nominal shear stress is 11 ksi. The average shear stress from the finite element analysis is 10.5 ksi on plane A. Note that the top edge distance to the cope, along plane A, does not contribute much in developing vertical shear stress.

This might be of interest relative to effect of radius on copes

Case 2, shown in Fig. 4.7, is similar to case 1; only the stiffness of the connection plate was increased. The stiffer connection forced more of a trapezoidal tensile stress distribution, but the stress distribution is still not uniform along the horizontal plane. The shear stress distribution on the vertical plane is similar to case 1. In cases 3 and 4 the end distance was increased eventually to 2 in. as shown in Figs. 4.8 and 4.9. The shear stress distribution for these two cases is very similar to cases 1 and 2 and is in close agreement with $\tau_{avg} = R / (d_n t_w)$. However, the tensile stress distribution along the horizontal plane is bilinear with a peak stress near bolt number 5.

The geometry of case 5 is similar to case 4, but one of the bolts was removed as shown in Fig. 4.10. The resulting vertical stress distribution appears to be the same as that of case 4; only a slight decrease of tensile stress is noticed at the end of the

beam near the connection for case 5. However, the peak stress and stress distribution in the tensile plane between bolt holes, commonly referred to as the gage, is of the same value.

To model case 6, the 4-bolt arrangement with a 2 in. end distance was again used, but instead of a 6 in. bolt spacing there was a 3 in. bolt spacing. The results of the vertical stress distribution shown in Fig. 4.11 indicates the same type of bilinear tensile stress distribution on the horizontal plane, but the peak tensile stress has increased. Also, the tensile plane between bolt number 4 and the end of the beam has a higher average tensile stress. The shear stress distribution on the vertical plane is not quite as uniform as compared to previous cases, but the value of $\tau_{avg} = 11$ ksi is close to representing the average shear stress. Figure 4.12 shows case 7 with the 4-bolt arrangement with a 2 in. end distance and the 9 in. bolt spacing. The shear stresses along the vertical plane are fairly uniform and close in magnitude to 11 ksi. The tensile stresses are lower in magnitude as compared to previous cases, being uniform between bolt holes with a slight peak near bolt number 4 and a decrease towards the end of the beam.

For case 8 the number of bolts was increased to 5 with the additional bolt being placed in the line of inside bolts to form a spacing of 3 in. The end distance remained at 2 in. The resulting vertical stress distribution shown in Fig. 4.13 is similar to the vertical stress distribution of case 5 and case 4. The shear stress distribution along the vertical plane between bolt holes is close to 11 ksi.

A 3-bolt arrangement with bolts spaced at 3 in. and a 2 in. end distance was used for case 9 (see Fig. 4.14). The resulting shear stress distribution along the vertical plane was less uniform with peak shear stresses near the bolt holes; the average shear stress is 14.6 ksi along the vertical plane and is greater than

11 ksi. The tensile stresses along the horizontal plane are of a definite bilinear distribution.

In examining the elastic behavior of the nine connections modeled, there appears to be a relationship between the end distance and the tensile stress distribution in the horizontal plane. The shear stiffness of the clip angle appears to cause the outside lower bolt (bolt number 5 in Fig. 4.15a), which is closest to the end of the beam, to pick up a large percentage of the shear in the connection. When the end distance is approximately 1 in. the tensile stress distribution in the horizontal plane is almost triangular; if the end distance is increased, the tensile stress distribution becomes bilinear and can be simulated by a bilinear stress distribution. This would seem especially reasonable for the connections that have smaller bolt spacings similar to case 6 where the high tensile stress concentration in the horizontal plane caused the resulting stress distribution to have a definite bilinear-type shape. The vertical shear stress appears to correlate with the shear stress obtained by dividing the reaction by the area of the web, except for the single row arrangement (case 9). The simulated vertical stress distributions are shown in Figs. 4.15a and 4.15b.

The spacing of the bolts also appears to have an effect on the vertical stress distribution. The contribution of forces on the horizontal tensile plane and vertical shear plane to the total vertical reaction of the double row connection varies as the bolt spacing is spread out or compacted and is also a function of the stiffness of the clip angles. For case 1, consisting of a flexible clip angle and a 6 in. deep connection, the horizontal tensile plane carried 51 percent of the total connection vertical reaction and the vertical shear plane carried the remaining 49 percent. With the more stiff clip angle and a 6 in. deep

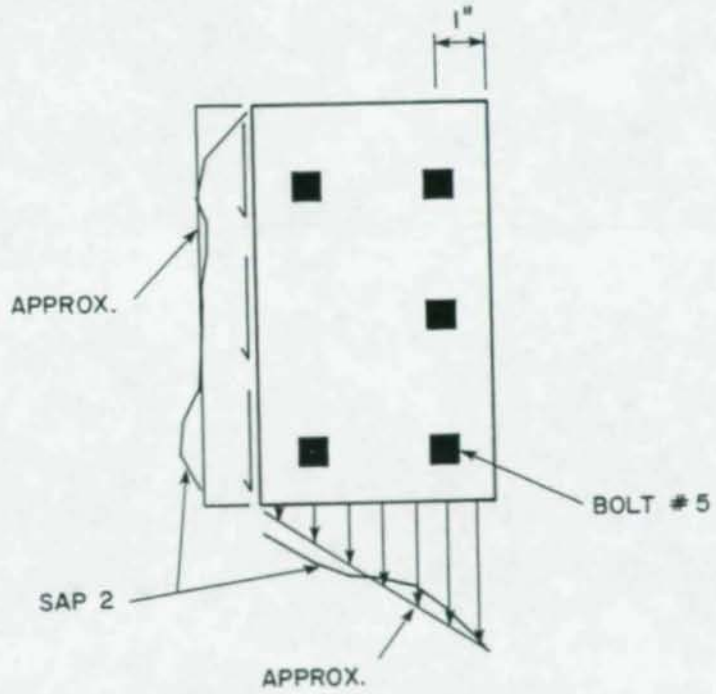


Fig. 4.15a Stress distribution for 1 in. end distance

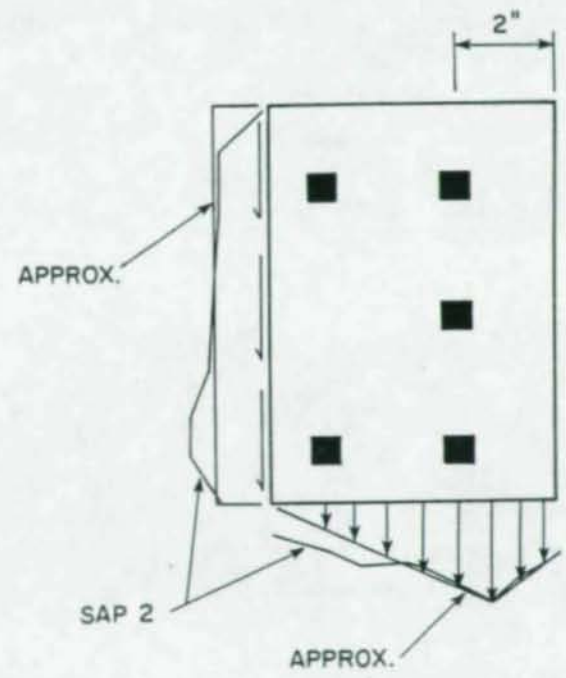


Fig. 4.15b Stress distribution for 2 in. end distance

connection, the horizontal tensile plane carried about 45 percent and the vertical shear plane carried 55 percent of the total vertical reaction. This same ratio was true for the double row connections modeled with a stiff clip angle and a 6 in. deep connection and only varied by 1 or 2 percent when the bolt arrangement within the 6 in. depth of the connection was altered. As the connection was made more compact, the tensile plane supported a greater portion of the total vertical reaction. The 3 in. deep connection of case 6 shows the horizontal tensile plane carrying 65 percent of the reaction. When the bolts are spread out in the vertical direction the opposite will occur for the 9 in. deep connection shows the horizontal tensile plane contributing 29 percent to the total reaction. For the single row connection (Fig. 4.14) the horizontal tensile plane carried 33 percent of the total reaction.

The shear stresses on the horizontal plane are of the same magnitude as the shear stresses on the vertical plane. A typical horizontal stress distribution around the connection is shown in Fig. 4.16. Local effects due to the bolt holes and eccentricity effects probably caused the stress reversal along the vertical plane.

A typical horizontal stress distribution is plotted along the vertical plane at the cope (line C-C) in Fig. 4.17. The finite element model results are plotted along with the theoretical bending stresses based on simple beam theory. The moment of inertia used for the theoretical stresses was calculated using the reduced depth at the cope. The finite element model predicts bending stresses near the cope more than twice that using simple beam theory. Hence the assumption that plane sections remain plane does not seem valid when trying to predict these bending stresses; more discussion of this matter is given in Chapter 5.

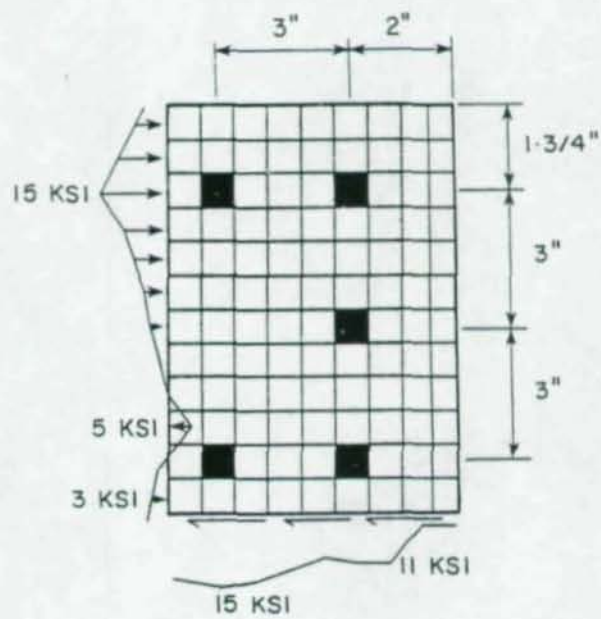


Fig. 4.16 Typical distribution of horizontal stresses

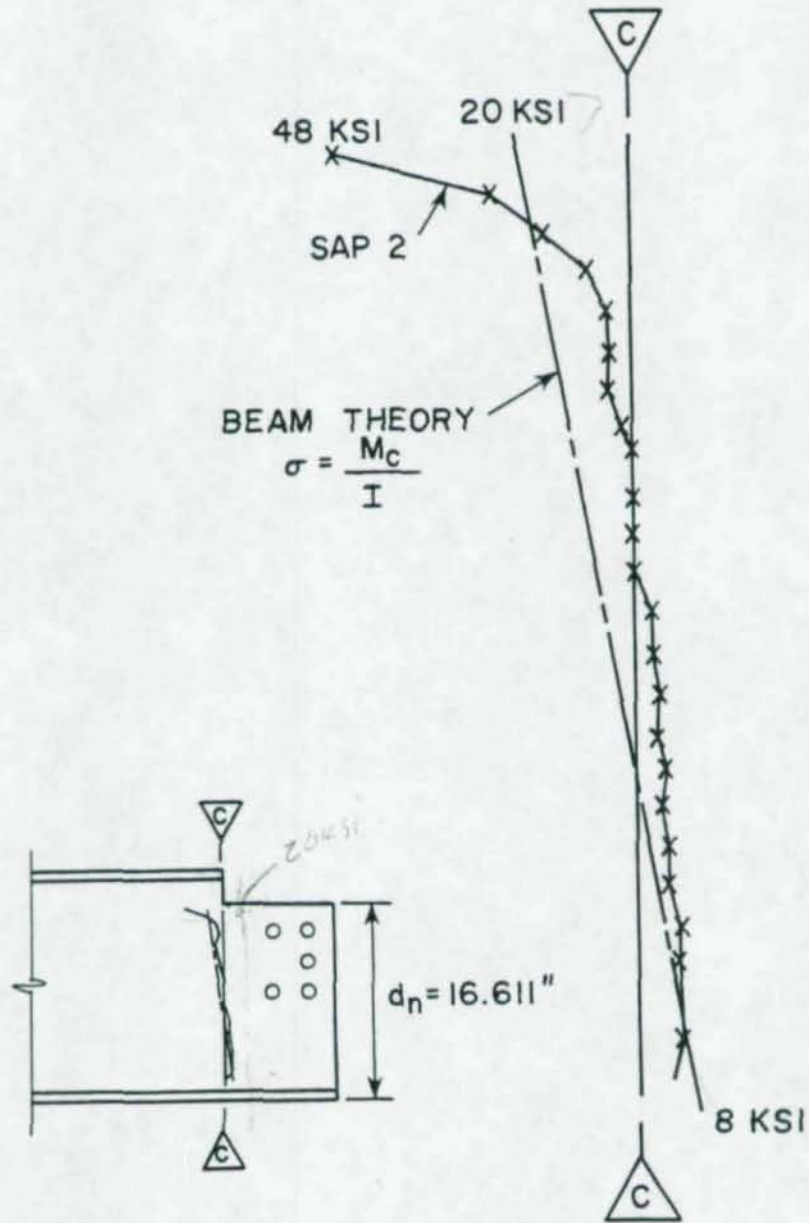


Fig. 4.17 Finite element and beam theory bending stress distribution at the cope

A summary of the finite element results indicate that the tensile stresses in the connection along the horizontal plane are a function of the depth of the connection, stiffness of clip angles, and end distance. The shear stresses developed along the vertical plane at the connection are not greatly affected by the depth of the connection. A stiffer pair of clip angles causes a more uniform reaction among all the bolts, forcing more of the reaction to be carried by the interior column of bolts close to shear plane A (shown in Fig. 4.6) compared to flexible clip angles. A failure model developed from the results of this chapter are compared to test results in Chapter 5.

CHAPTER 5

DISCUSSION OF TEST RESULTS AND
DESIGN RECOMMENDATIONSEffect of End and Edge Distance

All the tests appeared to have the same type of failure; fracturing of the web along the bottom line of bolts with yielding in the vertical plane between bolts. This is similar to the block shear failure described in Chapter 1. The capacity of the connection was affected by the end distance and edge distance.

Figures 5.1 and 5.2 show for all tests superimposed plots of the net deflection at the connection (difference between dial 1 and dial 2, see Fig. 2.5) versus the connection reaction R . The various end distances and edge distances for the bolt holes not only affects the capacity, but also the net vertical movement at the connection. The curves display similar behavior up to the start of fracturing; once fracturing commences the curves show individual behavior. Fracture of the web occurred at the same deformation for tests all in the same heat; Figs. 5.1 and 5.2 indicate the amount of deformation. Figure 5.1 indicates that with increased end distance the connection provides a higher capacity and a greater deformation capacity once fracture starts; webs with slotted holes showed an immediate decrease in capacity when fracture occurs. When a connection had the 1 in. minimum end distance, such as test 18-10, the capacity also decreased immediately after fracturing started. Test 18-12, which had a 2 in. end and edge distance, performed better than the uncoped test 18-13 which had a 1 in. end distance. Figure 5.2 indicates that the additional bolt in test 18-19 caused no difference in

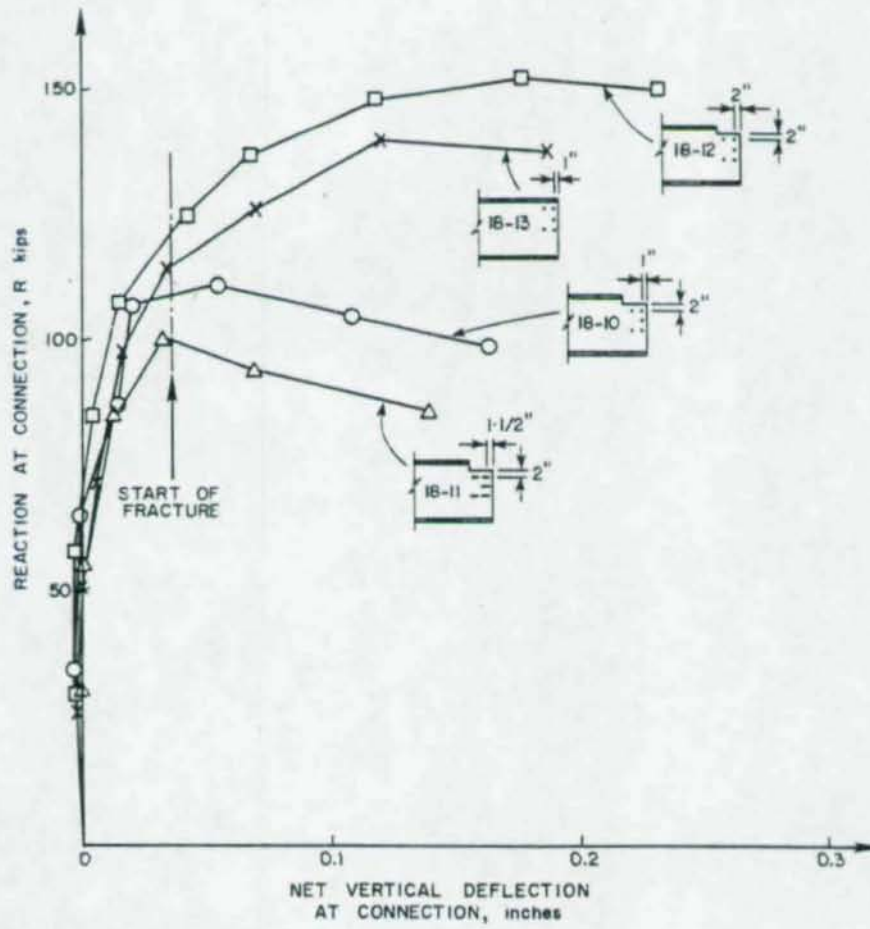


Fig. 5.1 Connection reaction versus net deflection at the connection for specimens of heat 1

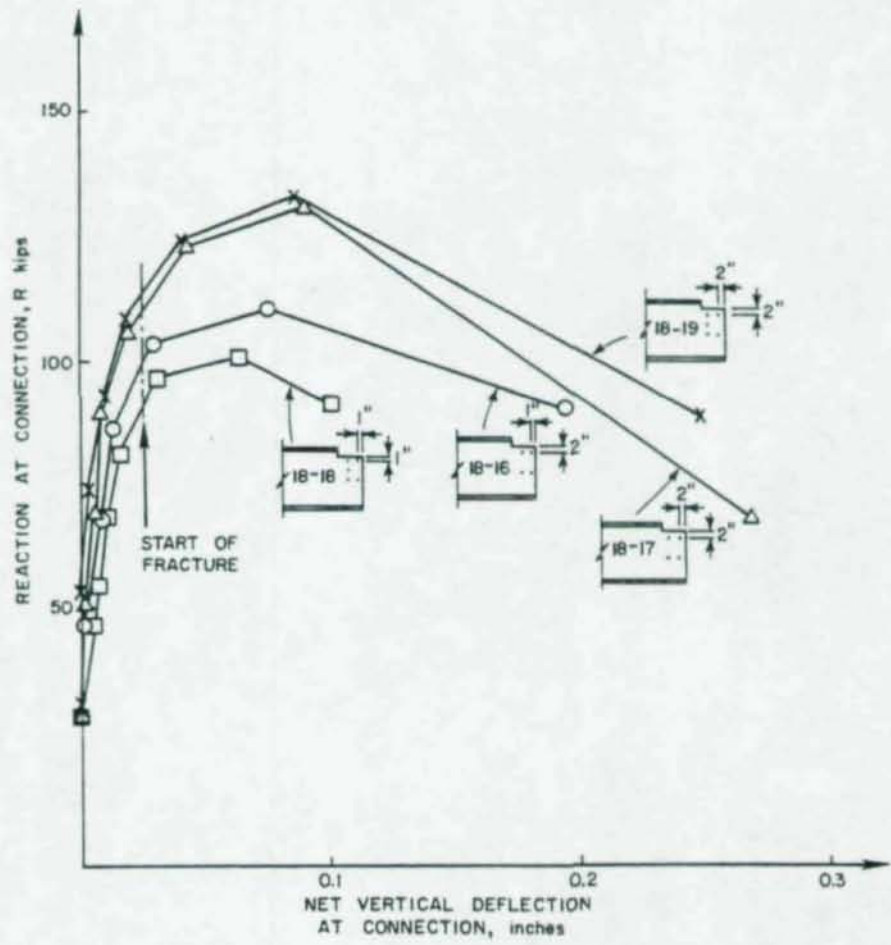


Fig. 5.2 Connection reaction versus net deflection at the connection for specimens of heat 2

behavior compared to test 18-17; however, the 5-bolt arrangement of test 18-12 improved the deformation capacity and strength of the connection. Tests 18-12, 18-17, and 18-19 all had the same 2 in. end and edge distance. The elastic stress distribution from the finite element models in Chapter 4 were shown to be similar for these three tests, hence, the difference in capacity is related to the behavior once yielding and fracture starts. ↓ ?

The distribution of vertical reaction between the two rows of bolts is a function of the clip angle stiffness as indicated in Chapter 4; fracture along the bottom line of bolts is initiated at the bolt hole closest to the end of the beam and progresses along the horizontal plane. Comparing the curves of test 18-12 with 18-16 and 18-17 in Figs. 5.1 and 5.2, the fracture load is not affected by the different bolt arrangements of these connections. Figure 5.2 also shows that the larger edge distances increase the connection capacity, but not as effectively as end distance. This is evident by comparing test 18-16 with 18-17 where the end distance was varied by 1 in., and an 18 percent increase in capacity was obtained. When increasing the edge distance by 1 in., (tests 18-16 and 18-18), the capacity was increased only by 9 percent. Tests 18-18 and 18-19 show the difference in capacity when increasing both the end distance and edge distance. The tests which had a 2 in. end distance and/or edge distance were able to develop more shear in the web of the beam (away from the connection) than tests with minimal end and edge distance.

AISC Allowable Connection Capacity

In Table 5.1 a summary of the AISC allowable reactions, based on the 1978 AISC Specification, and factors of safety are given for each test. In column 1 of Table 5.1 the allowable reaction is given based on a shear stress of $0.4F_y$ over the web area, $d_n x t_w$. The bolt shear strength (column 2) is the shear

TABLE 5.1 AISC ALLOWABLE REACTION

HEAT 1

$t_w = 0.44$ in. $F_y = 38.3$ ksi
 $F_u = 59.7$ ksi

Test Number	Allow. Web Shear (kips)	AISC Allowable Reaction							R_{allow} (kips)	R_u (kips)	Factor of Safety
		Bolt Shear (kips)	Bolt Bearing (kips)	Top Edge Distance (kips)	Eccentricity Factor-1980	Eccentricity Factor-1978	End Distance (kips)	Block Shear (kips)			
18-10	113	133	148	131	0.60	0.75	62	87	62	111	1.79
18-11	114	133	148	131	0.60	0.75	62	74	62	101	1.63
18-12	113	133	148	127	0.60	0.75	131	101	76	152	2.00
18-13	123	133	148	--	0.60	0.75	62	--	62	140	2.26

HEAT 2

$t_w = 0.43$ in. $F_y = 36.6$ ksi
 $F_u = 58.0$ ksi

Test Number	Allow. Web Shear (kips)	AISC Allowable Reaction							R_{allow} (kips)	R_u (kips)	Factor of Safety
		Bolt Shear (kips)	Bolt Bearing (kips)	Top Edge Distance (kips)	Eccentricity Factor-1980	Eccentricity Factor-1978	End Distance (kips)	Block Shear (kips)			
18-16	106	106	112	103	0.60	0.67	56	86	56	111	1.98
18-17	106	106	112	106	0.60	0.67	97	96	64	131	2.05
18-18	106	133	140	62	0.51	0.62	70	72	32	101	3.16
18-19	106	133	140	125	0.51	0.62	121	89	64	134	2.09
	(1)	(2)	(3)	(4)	(5)	(6)	(7)	(8)	(9)	(10)	(11)

88988

strength of the bolts considering no eccentricity effect. The bolt bearing strength in column 3 is based on the upper limit for bearing stress (Eq. (1.4) in Chapter 1). The allowable reaction based on the bearing stress formula for top edge distance (Eq. (1.5) in Chapter 1) appears in column 4; the value in column 4 is based on having all the bolts' bearing strengths equal to that of the bolt with the minimum top edge distance as implied by the Specification.¹ The end distance in column 7 is the allowable reaction based on the bolt bearing strength (Eq. (1.6) in Chapter 1) of the most critical bolt and applied to the other bolts. Column 8 lists the allowable reactions based on a block shear failure (Eq. (1.7) in Chapter 1).

The 1978 AISC Specification requires ^{? permits} that the effect of eccentricity be neglected when determining the reaction based on end distance (column 7 of Table 5.1). However, it is not clear in the 1978 AISC Specification whether the effect of eccentricity should be considered when determining reactions based on bolt bearing and edge distance (columns 3 and 4 of Table 5.1). The author will interpret the 1978 AISC Specification so as to consider any eccentricity that may exist and apply it to bolt bearing and edge distance. In the seventh edition of the AISC Manual,¹⁵ the approach recommended by Higgins⁹ was adopted for eccentricity effects; the eighth edition of the AISC Manual¹⁶ recommends Crawford and Kulak's approach.⁸ Higgin's approach assumes elastic behavior and replaces the actual eccentric arm with an effective eccentricity; Kulak's approach developed the concept of an ultimate strength method which assumes an instantaneous center of rotation of the connection with the actual eccentricity. The 1980 eccentricity factor in column 5 of Table 5.1 is based on Kulak's approach while the 1978 eccentricity factor in column 6 is based on Higgin's approach. The eccentricity factors represent the reduction in capacity due to

the eccentricity of the shear load, which was assumed to be equal to the distance from the face of the column stub to the centroid of the fastener group. This factor follows the procedure in the eighth edition of the AISC Manual. As implied by the 1978 AISC Specification, the eccentricity factor was multiplied by the bolt shear, bolt bearing and top edge distance bearing strength to determine the allowable reaction.

Kulak's method produced the smallest value of eccentricity factor in all cases. This method was chosen instead of Higgin's approach for calculating the allowable reaction which appears in column 9 of Table 5.1. The allowable reaction is the smallest reaction in columns 1 through 8 after the eccentricity factor is applied to columns 2 through 4. The ultimate reaction during the tests appears in column 10 with the factor of safety against failure (column 10 divided by column 9) appearing in column 11.

Considering the Effect of Eccentricity

In Table 5.1 the eccentricity factors discussed previously are all greater using Higgin's elastic approach compared to Kulak's ultimate method. Higgin's approach produces a larger eccentricity factor because the actual eccentricity is replaced with a reduced effective eccentricity; Kulak's approach uses the actual eccentricity. Kulak's method is sensitive to the degree of eccentricity; if the actual measured eccentricity is used from Fig. 3.8 at the start of fracture in the connection, then the eccentricity factor is increased to 0.83 from the previous value of 0.60. The allowable load is directly proportional to the eccentricity factor. Test 18-12 has a capacity of 95 kips if Higgin's approach is used, leaving a factor of safety of only 1.59, whereas the factor of safety is 2.0 based on Kulak's approach.

In some instances the factors of safety were satisfactory (2.0 or greater) because the eccentricity factor based on Kulak's approach was used to modify the edge distance bearing stress formula (Eq. (1.5)) which was assumed to limit the bearing load for all bolts in the particular connection. As a result of using the eccentricity factors the factors of safety were satisfactory for cases that would otherwise be unsatisfactory. The eccentricity factors have thus provided a margin of safety against a failure not caused by eccentricity but by block shear for the compact connections. The eccentricity factors are based on bolt strength, not bearing strength of the material surrounding the bolt. It is the opinion of the author that the eccentricity factors are only valid for bolt strength and need to be investigated for cases when a bearing failure controls. Tests herein did not examine the effects of varying the eccentricity by a significant amount; more work should be done to determine the effect eccentricity may have on block shear type failures.

Connection Capacity Controlled by
End or Edge Distance

The philosophy of the AISC Specification is to have a factor of safety of at least 2.0 in connection design. The results show three tests with unsatisfactory factors of safety. The controlling parameter for the tests was either end distance considering no eccentricity or edge distance with the applied eccentricity factor. The mode of failure for all the tests was not edge or end tear out of the bolt, but rather a block shear failure. The end and edge distance formulas are based on the bolt shearing along two planes, planes A-A and B-B as shown in Fig. 5.3. Although the tests reported herein did not fail due to edge distance problems because of block shear being critical, other tests have indicated edge distance effects.^{17,18}

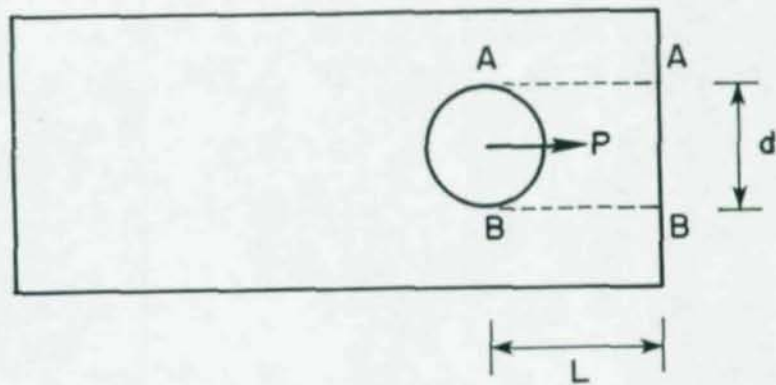


Fig. 5.3 Model for basis of bearing stress formula

When examining the horizontal plane of fracture between the bottom bolt and the end of the beam, necking along the fracture was noticed, hence the fracture was due mainly to a tensile force and not a shear force. The elastic finite element model also showed low shear stresses along the horizontal plane of fracture. No fracture or hole elongation of the web occurred between the top bolt holes and the edge of the cope, however, the bearing stress formula based on top edge distance (Eq. (1.5)) controlled the allowable reaction of four tests (see Table 5.1).

Block Shear

The block shear model currently in the 1978 AISC Specification does not seem valid for double row connections. A block shear failure was not predicted by the formulas, yet it occurred. The factors of safety for the tests assuming that block shear (Eq. (1.7)) did control, are listed in Table 5.2. The factor of safety, which in every instance is less than 2.0, is not at a satisfactory level. Most of the tests have a satisfactory factor of safety listed in Table 5.1 because the capacity is controlled by a conservative edge distance or end distance interpretation of the 1978 AISC Specification. If the end and edge distances are increased and eccentricity ignored, the factor of safety would be less than 1.51 as given by tests 18-12, 18-17, and 18-19 in Table 5.2.

The current block shear model needs to be revised in order to give satisfactory factors of safety based on actual failure. The block shear failure model referenced in Chapter 1 assumed full tensile strength along the horizontal plane between the bottom line of bolts and full shear strength along the vertical plane (see Fig. 1.5). The elastic finite element model showed that the tensile stress distribution was nonuniform over the horizontal plane with high stresses near the lower bolt close to

TABLE 5.2 1978 AISC ALLOWABLE REACTION
BASED ON BLOCK SHEAR

Test Number	Block Shear (kips)	R_u (kips)	Factor of Safety
18-10	87	111	1.28
18-11	74	101	1.36
18-12	101	152	1.50
18-13	--	140	--
18-16	86	111	1.29
18-17	96	131	1.36
18-18	72	101	1.40
18-19	89	134	1.51

the beam's end. From tests, it is known that fracture first occurs in this area of the horizontal plane (see Fig. 5.4.). No signs of shear fracture along the vertical plane were observed in the tests, rather there was gross yielding along the vertical plane previously discussed in Chapter 3 and in Fig. 3.11.

To predict the connection capacity for block shear a new failure model based on the tests and analysis herein is shown in Fig. 5.5. A triangular tensile stress distribution along the horizontal plane is recommended; this linear approximation of stress distribution is based on the finite element analysis with an end distance of 1 in., and gives conservative results when the end distance is greater than the minimum required. The capacity of the net section along the horizontal failure surface should be considered to be effective in tension. The vertical plane in the connection after failure showed no fracture due to shear, but

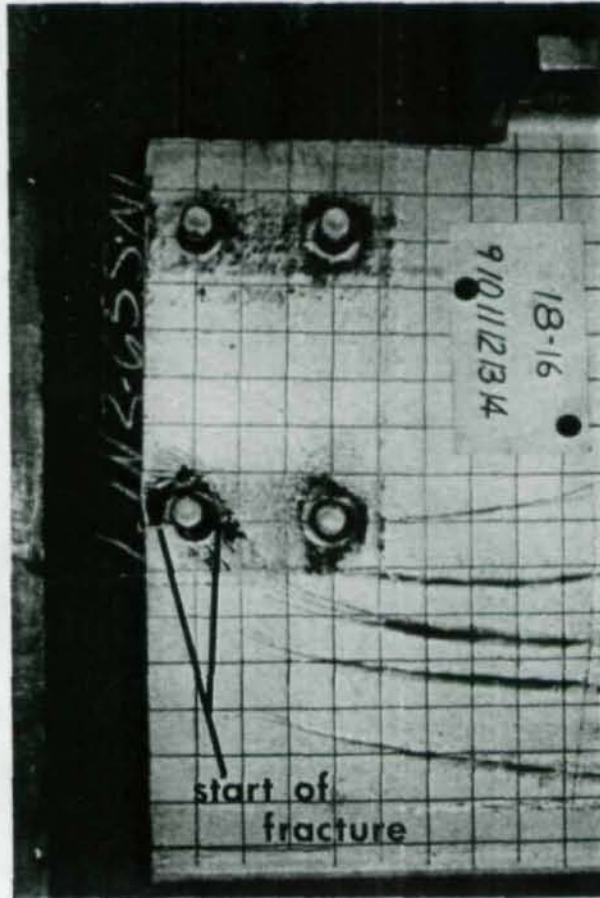


Fig. 5.4 Area of web where fracture first occurs

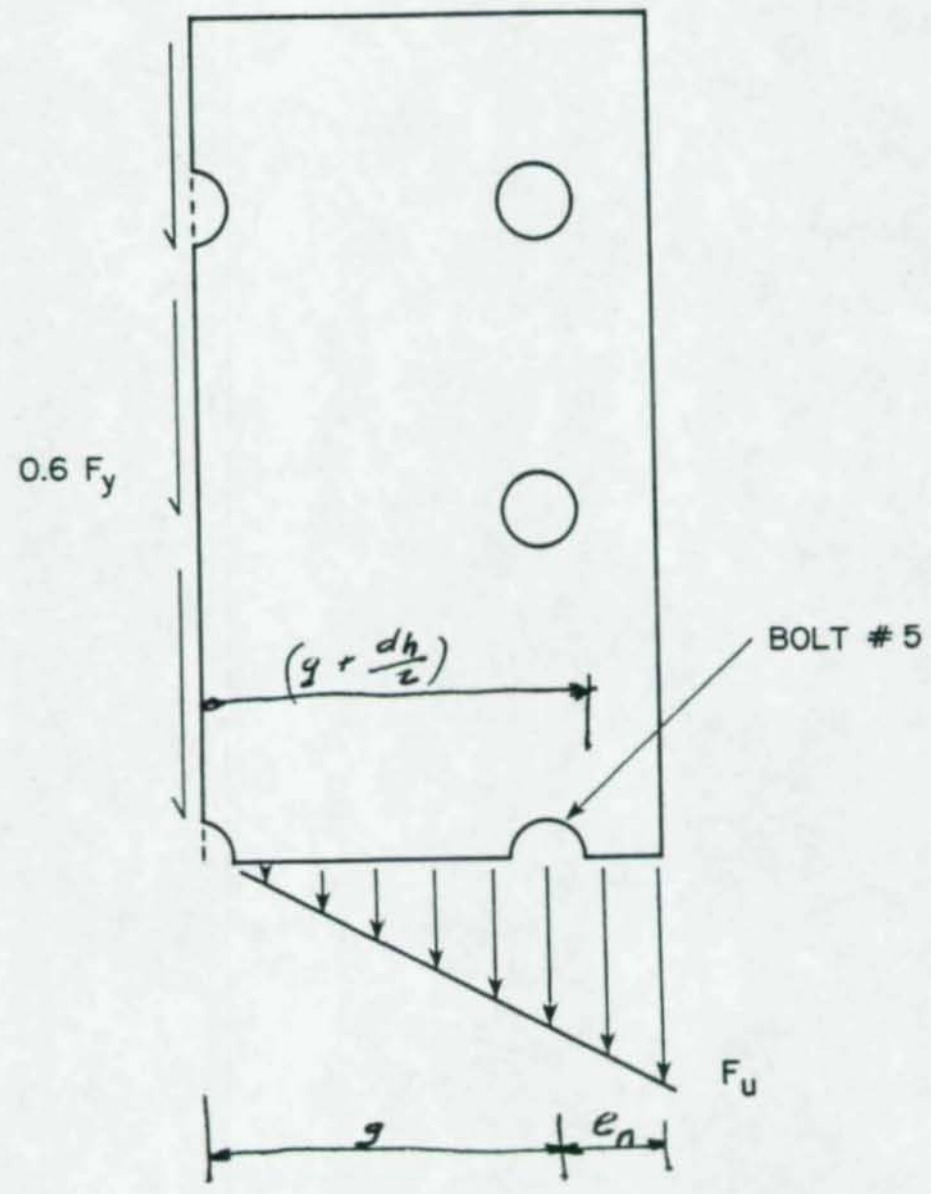


Fig. 5.5 New failure model for block shear

rather gross yielding. The Von Mises yield criterion is assumed where yielding occurs as the shear stress reaches a value of $F_y/\sqrt{3}$, which is approximately $0.6F_y$. The gross section along the vertical plane in the connection between the bottom row of holes and the top of the beam is assumed to develop a shear stress of $0.6F_y$. The capacity of a connection against block shear based on the new failure model would be:

Block Shear Capacity = Tensile Strength + Shear Yielding

$$R_u = F_u \left[\left[g + e_n \right] t_w \times \frac{1}{2} - \left[\frac{g + d_h/2}{g + e_n} \right] t_w d_h \right] + 0.6F_y \left[e_g + \sum s \right] t_w \quad (5.1) \quad ?$$

For the case where an uncoped beam has a compact connection (test 18-13), the new block shear failure model will predict when the start of fracture occurs, assuming the uncoped compression flange does not carry any vertical shear. The start of fracture occurred during test 18-13 at approximately 115 kips (see test 18-13 of Appendix I) the new block shear model gives a capacity of 121 kips. The load at which fracture of the web starts should be considered the maximum serviceable load because with any increase in the load the deformations become large. Table 5.3 lists a summary of ultimate loads and capacities predicted by the new failure model for each test. The allowable load is based on the block shear capacity with a factor of safety of 2.0.

The nonuniform tensile stress along the horizontal plane discussed previously is a result of the bolt near the beam's end (bolt number 5 in Fig. 5.5), carrying a large percentage of the connection's reaction R and creating stress concentrations near this bolt hole. As the connection is made deeper, the vertical shear plane will develop more shear and the contribution of the horizontal tensile plane will reduce (case 7 of the finite element

TABLE 5.3 REACTION CAPACITY BASED ON NEW
BLOCK SHEAR FAILURE MODEL

Test Number	Block Shear Capacity R_f (kips)	R_u (kips)	$\frac{R_u}{R_f}$	R_{allow} (kips)
18-10	113	111	0.98	57
18-11	106	101	0.95	53
18-12	130	152	1.17	65
18-13	121	140	1.16	61
18-16	109	111	1.02	55
18-17	123	131	1.07	62
18-18	99	101	1.02	50
18-19	122	134	1.09	61

analysis). As a result, the stress distribution along the horizontal plane becomes more uniform and the stress concentrations disappear. A block shear failure can be avoided by developing a greater depth of the beam's web at the connection.

Stability of the Web

The high horizontal compressive stresses in the web, as shown in Fig. 4.17, can cause the web to buckle at the cope. This was witnessed in a few tests as shown in Fig. 5.6. According to the AISC Structural Steel Detailing Manual,¹⁹ it is suggested that the bending stresses at the cope (line C-C in Fig. 4.17) be calculated using the section properties at the reduced depth and then compared to the allowable bending stress, $0.6F_y$. The AISC Structural Steel Detailing Manual makes no reference to a stability check of the beam's web. From the elastic finite element analysis, shown in Fig. 4.17, the theoretical bending stresses

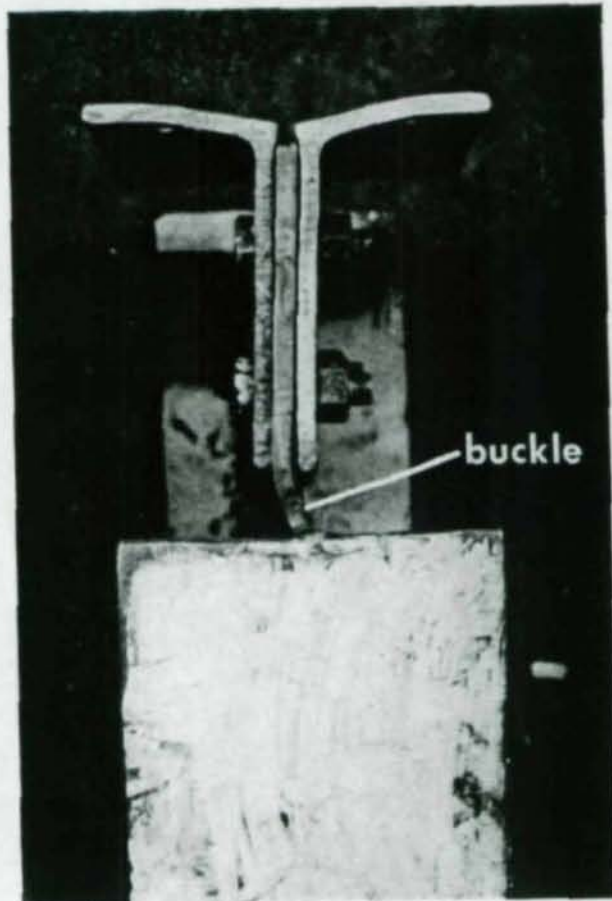


Fig. 5.6 Top view of beam showing a buckle in the web at the cope

predicted by beam theory were smaller by a factor of two. Obviously there is some discrepancy since the AISC approach gave calculated bending stresses which were less than $0.6F_y$; however, yielding and buckling occurred. It may not be sufficient to compare the bending stresses calculated using beam theory with a stress of $0.6F_y$. The connection's capacity may be controlled by buckling of the web at the cope when the cope becomes long. Further research should be done to establish a method of checking the stability of the web in coped connections.

The placement of a compact connection with respect to beam depth is significant for the stability of coped and uncoped connections. Test 18-13 indicated that if the compression flange is uncoped, then there is restraint against vertical deformation of the web at the connection. This will result in compressive stresses in the web directly above the connection. Consequently, the web may yield and buckle in this zone. A connection such as the one shown in Fig. 5.7 will prevent a block shear failure, however, failure may occur by web buckling above the connection. Therefore, any connection with this type of detail should be avoided unless the web is checked for stability.

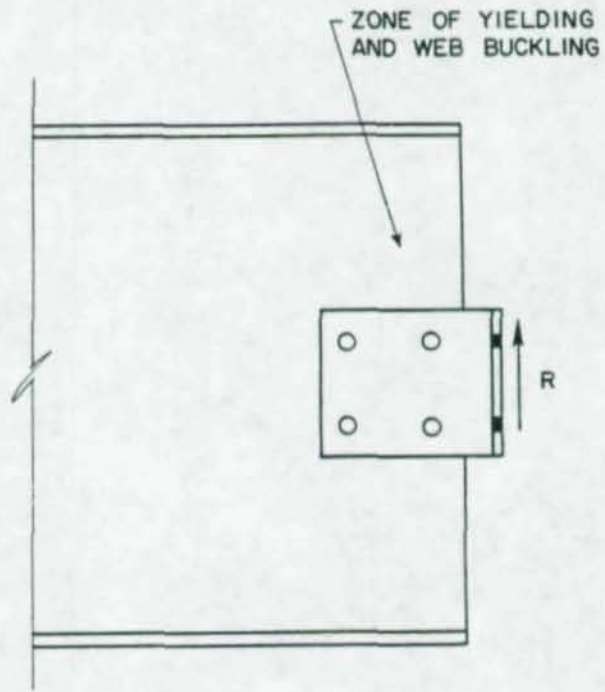


Fig. 5.7 Compact connection placed at a lower depth

CHAPTER 6

SUMMARY AND CONCLUSIONS

A research program was carried out to study the behavior of double row bolted shear connections. The program consisted of full-scale testing of eight W18x60 beams of A36 steel and also of analytical studies using an elastic finite element program. Interacting factors such as minimum end and edge distance, double row of bolts, and type of hole (standard or slotted) were investigated. The results show that:

(1) All the connections behaved the same with failure initiated by fracturing of the web along the bottom horizontal line of bolts followed by yielding in the web between the plane of fracture and the top of the beam, compression flange, at the connection. This type of failure is called a block shear failure.

(2) A few of the beams had the web yield and buckle at the cope after the web had fractured and the connection had undergone large deformations.

(3) The eccentricity of the connection varies as the connection load is increased.

(4) The one test with slotted holes showed a 9 percent decrease in capacity due to less area in the horizontal tensile plane.

(5) End distance is more critical in the connection than edge distance due to the concentration of tensile stress at the bolt closest to the beam's end along the bottom line of bolts. The tensile stress distribution is nonuniform along the horizontal plane; the shear stresses are uniform along the vertical plane.

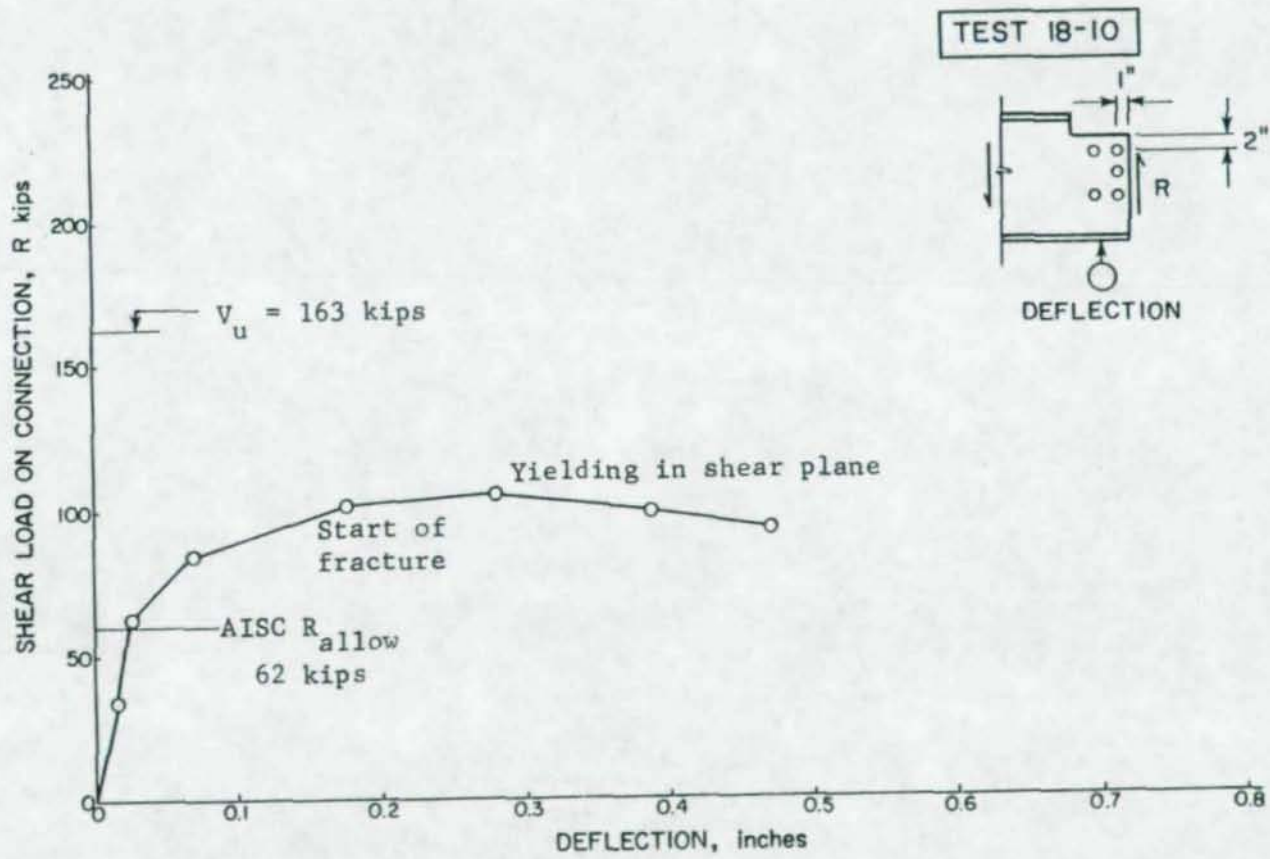
(6) The current 1978 AISC Specification does not predict block shear failures for the tests, yet they occurred. The allowable capacity of the connections was controlled either by the edge distance bearing stress formula (Eq. (1.5)) or the end distance bearing stress formula (Eq.(1.6)) with an applied eccentricity factor to consider the effects of eccentricity. The factor of safety was sometimes unsatisfactory.

(7) A new block shear failure model (Eq. (5.1)), consisting of gross yielding on the vertical plane and a triangular tensile stress distribution along the horizontal plane, gives a satisfactory factor of safety of the connection capacity against a block shear failure (Table 5.3).

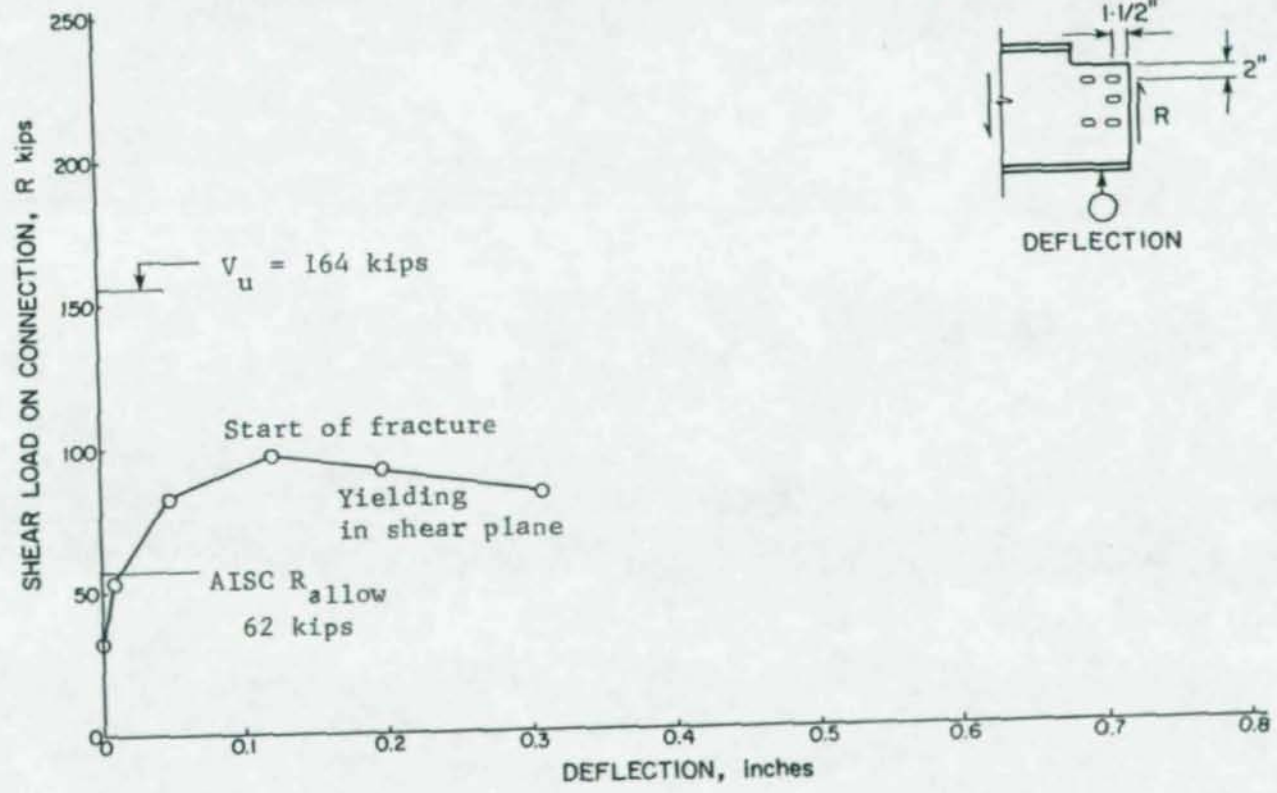
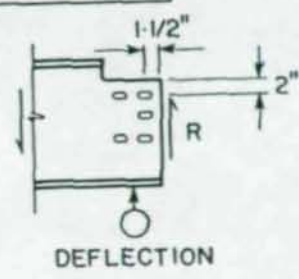
(8) The elastic finite element analysis shows the bending stresses at the cope to be twice as large as the bending stresses predicted by beam theory. Only checking the bending stresses against the stress of $0.6F_y$, as suggested by the Structural Steel Detailing Manual, is not satisfactory for the web at the cope may not be stable at this level of stress.

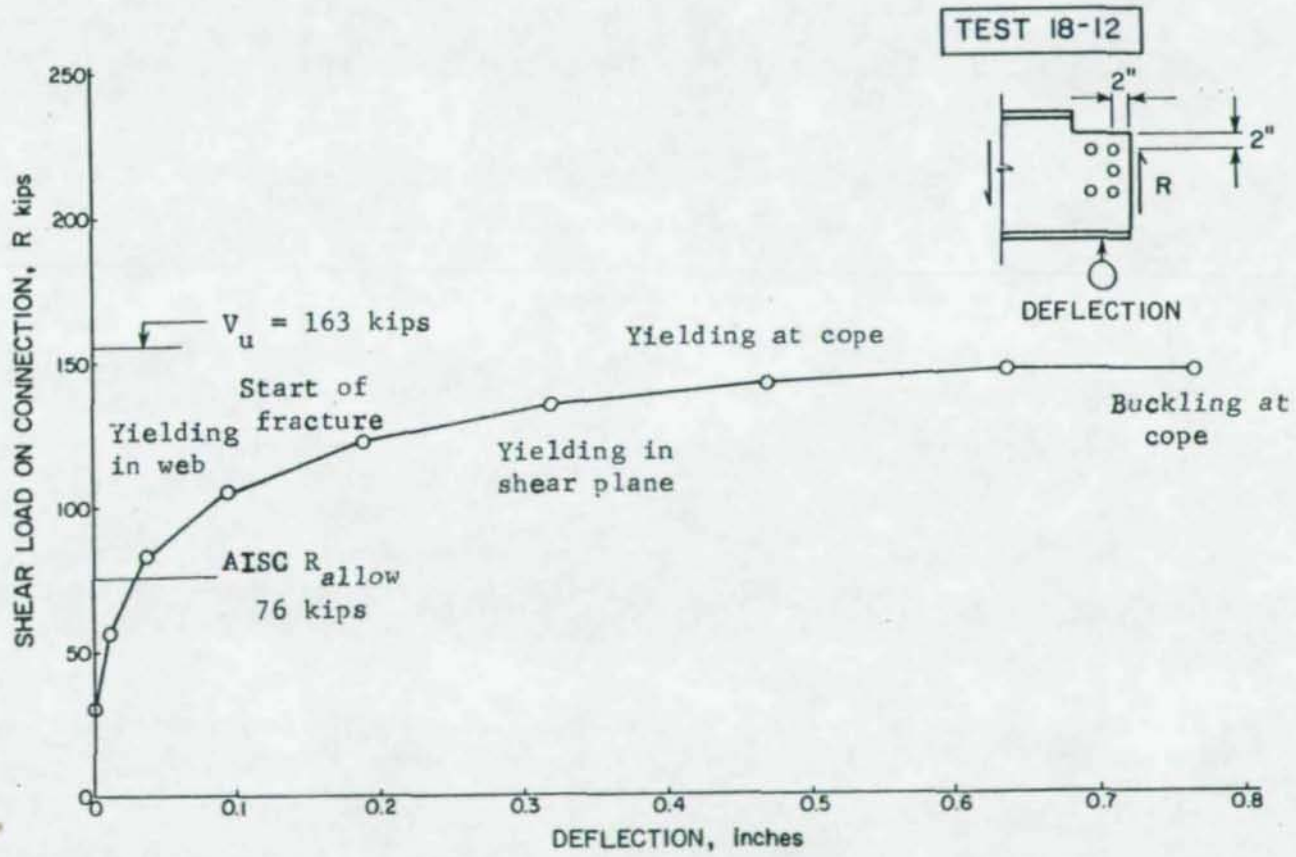
A P P E N D I X I

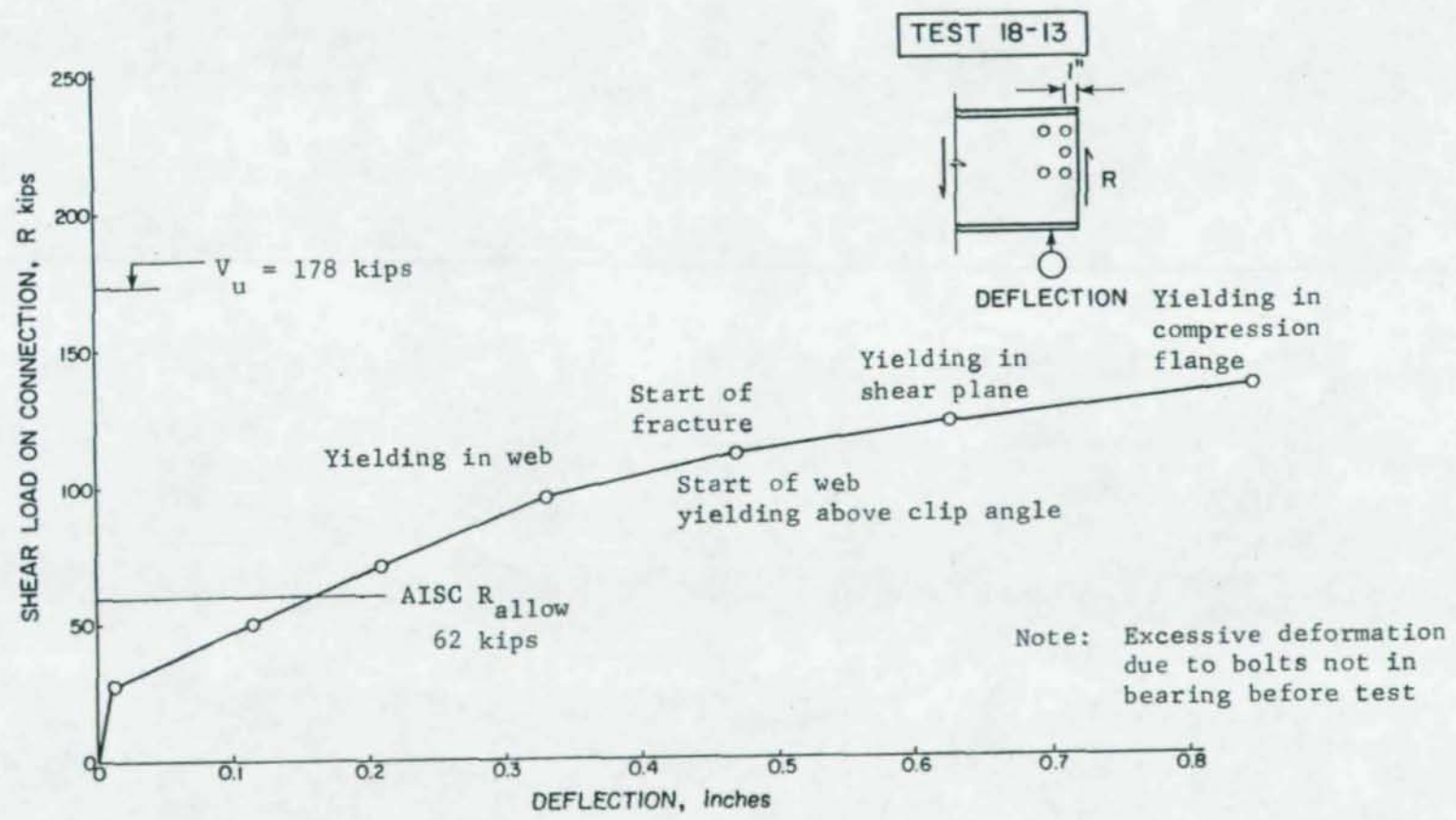
LOAD-DEFORMATION BEHAVIOR



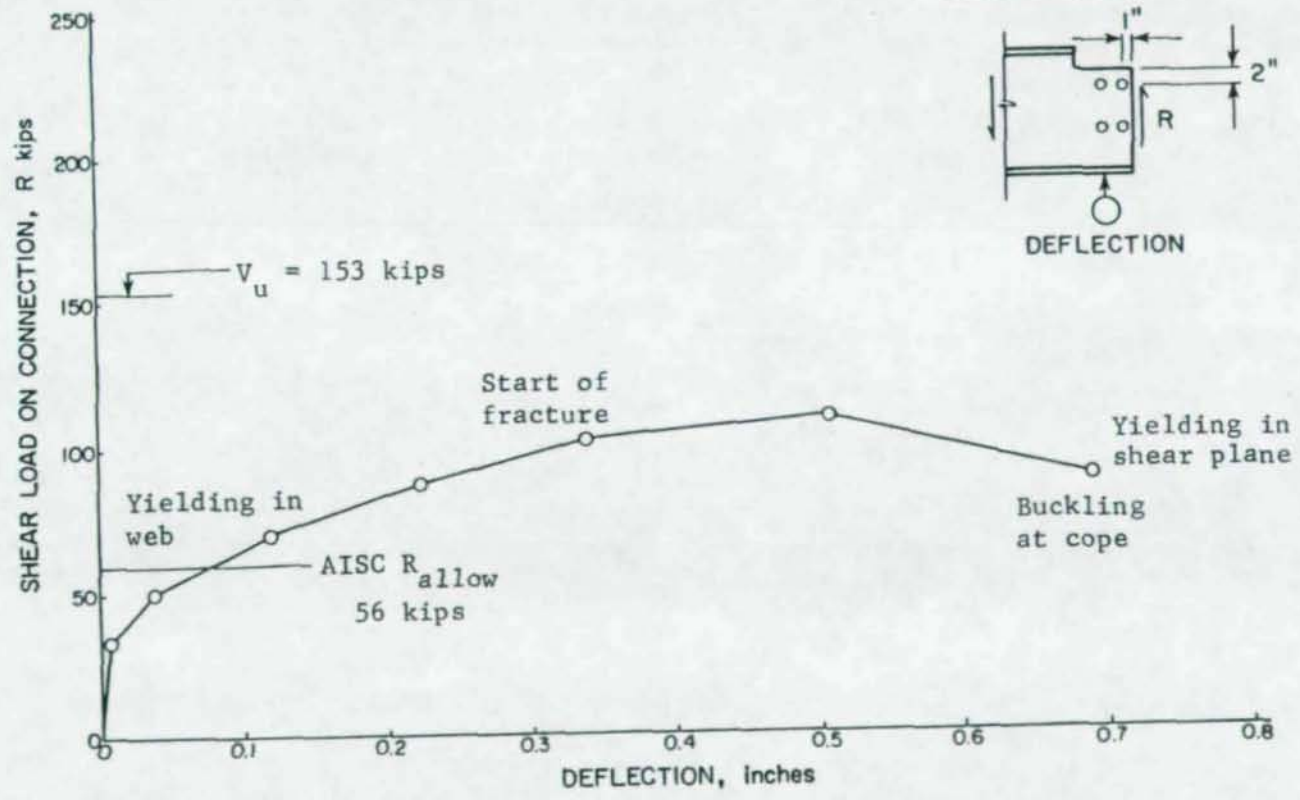
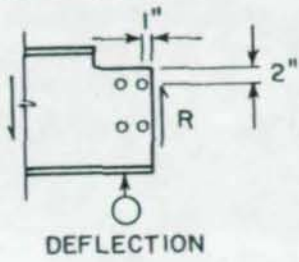
TEST 18-11

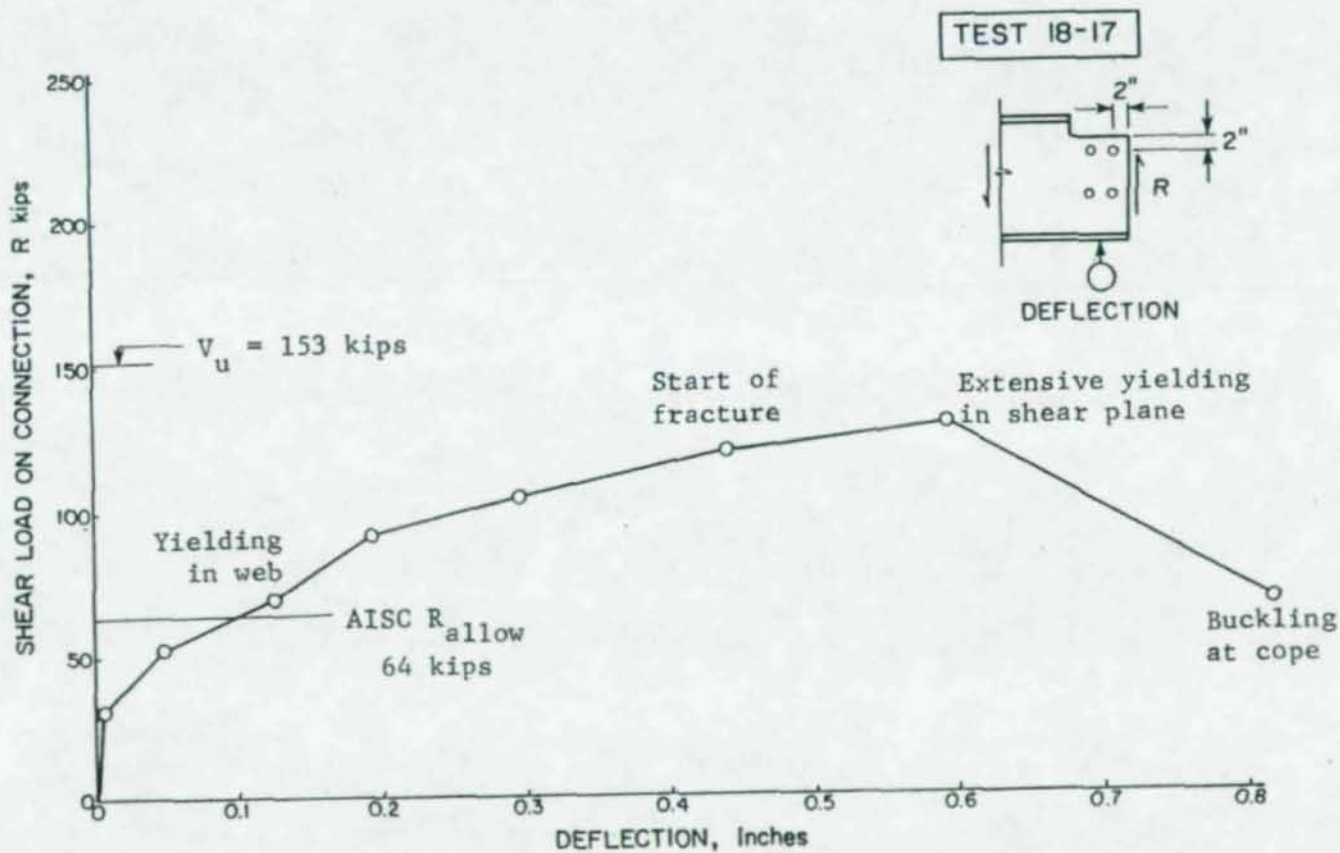




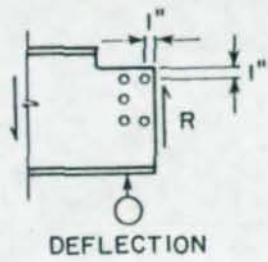
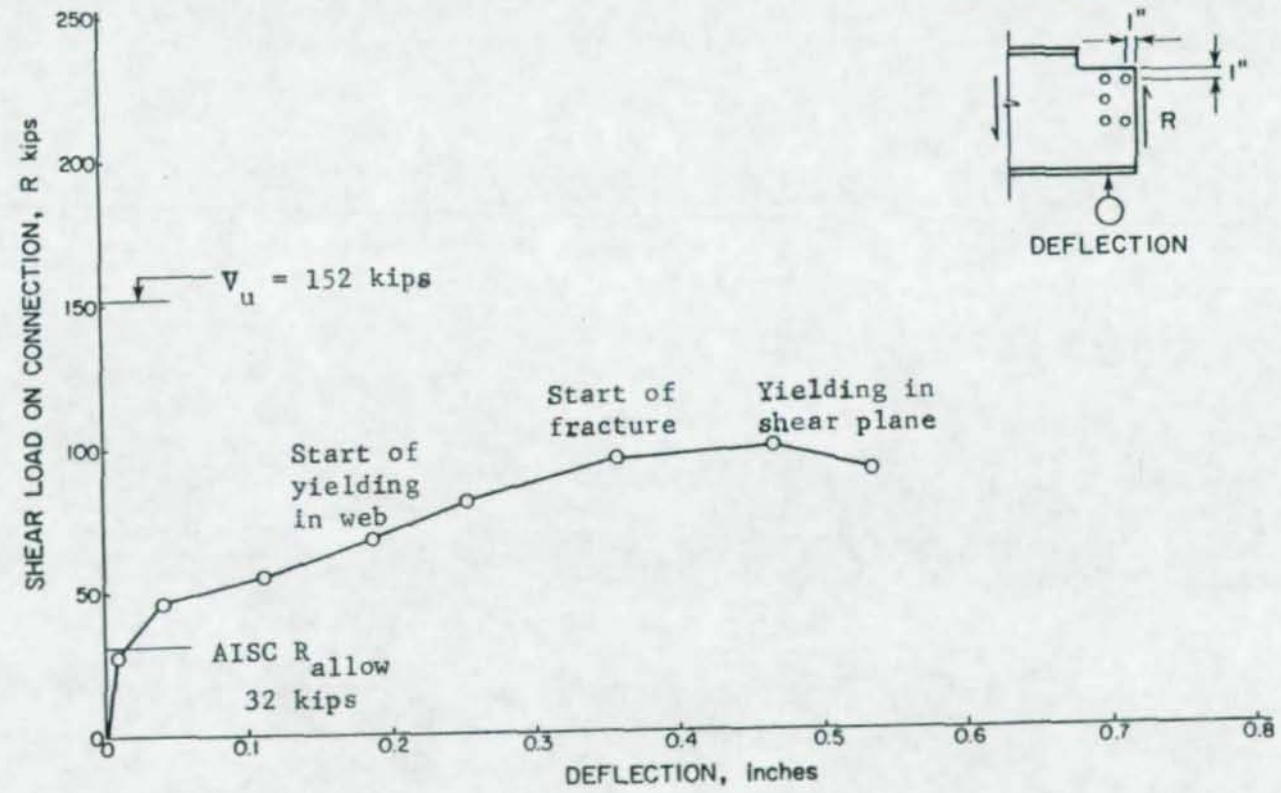


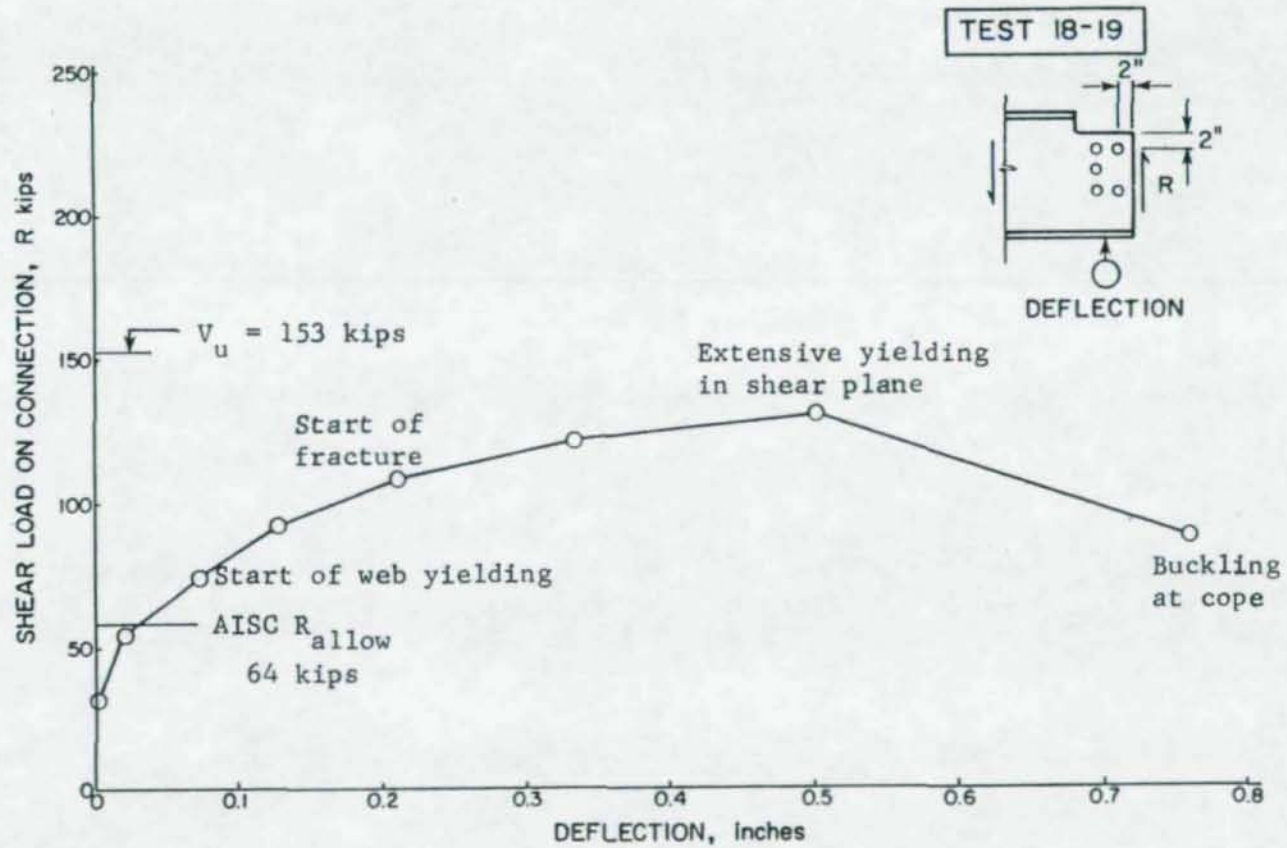
TEST 18-16





TEST 18-18





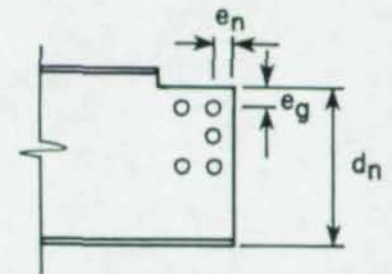
A P P E N D I X I I

REPRESENTATIVE DIMENSIONS OF SPECIMENS

TABLE II-1 AVERAGE REPRESENTATIVE DIMENSIONS

Test Number	End Distance e_n	Edge Distance e_g	Net Depth d_n	Web Thickness t_w
18-10	15/16	2	16-3/4	0.44
18-11	1-1/2	2	16-13/16	0.44
18-12	2	1-15/16	16-3/4	0.44
18-13	15/16	--	18-1/4	0.44
18-16	1-1/8	2-1/16	16-13/16	0.43
18-17	1-15/16	2-1/8	16-7/8	0.43
18-18	1-1/8	1	16-3/4	0.43
18-19	1-15/16	2	16-13/16	0.43

All dimensions in inches



A P P E N D I X I I I

SAMPLE CALCULATIONS FOR TEST 18-12

$$A_w = 7.37 \text{ in.}^2$$

$$F_y = 38.3 \text{ ksi}$$

$$d_n = 16.75 \text{ in.}$$

$$n = 5 \text{ bolts}$$

$$e_g = 1.938 \text{ in.}$$

$$s = 3.0 \text{ in.}$$

$$e_n = 2.0 \text{ in.}$$

$$t_w = 0.44 \text{ in.}$$

$$F_u = 59.7 \text{ ksi}$$

Von Mises Shear Yield Capacity

$$\begin{aligned} V_u &= \frac{F_y}{\sqrt{3}} A_w \\ &= \frac{38.3}{\sqrt{3}} 7.37 = 162.9 \text{ (kips)} \end{aligned}$$

Calculations to Determine
AISC Allowable Reaction

(a) Allowable Web Shear

$$\begin{aligned} V &= 0.4 F_y A_w \\ &= 0.4(38.3)(7.37) = 112.9 \text{ (kips)} \end{aligned}$$

(b) Bolt Shear Ignoring Effect of Eccentricity

$$\begin{aligned} P_b &= V_b n \\ &= 26.5(5) = 132.5 \text{ (kips)} \end{aligned}$$

(c) Bolt Bearing

$$P_p = F_p A_p n$$

where

$$F_p = 1.5 F_u$$

thus,

$$P_p = 1.5(59.7)(0.44)(0.75)(5) = 147.7 \text{ (kips)}$$

(d) Bolt Bearing Limited by Connection
Top Edge Distance

$$P_g = \frac{e F t}{2} n$$

$$= \frac{1.938(59.7)(0.44)}{2} (5) = 127.2 \text{ (kips)}$$

thus,

the allowable reaction based on bolt load applying the effects of eccentricity.

where

Kulak's eccentricity factor = 0.60

and

minimum allowable total bolt force = 127.2 (kips)

(Bolt force is controlled by bolt bearing limited from top edge distance)

is

$$R = 127.2(0.60) = 76.3 \text{ (kips)}$$

(e) Allowable Bolt Bearing Limited by
Connection End Distance

$$P_n = \frac{e F t}{2} n$$

$$= \frac{2.0(59.7)(0.44)}{2} (5) = 131.3 \text{ (kips)}$$

(f) Allowable Reaction Based on Block Shear

$$R = A_v 0.3F_u + A_t 0.5F_u$$

where

$$\begin{aligned} A_v &= [e_g + 2s - 1.5d_h] t_w \\ &= [1.938 + 2(3.0) - 1.5(3/4 + 1/8)] 0.44 = 2.92 \text{ (in}^2\text{)} \end{aligned}$$

and

$$\begin{aligned} A_t &= [g + e_n - 1.5d_h] t_w \\ &= [3.0 + 2.0 - 1.5(3/4 + 1/8)] 0.44 = 1.62 \text{ (in}^2\text{)} \end{aligned}$$

thus,

$$R = 2.92(0.3)(59.7) + 1.62(0.5)(59.7) = 100.6 \text{ (kips)}$$

thus,

the AISC Allowable Reaction is

$$R_{\text{allow}} = 76.3 \text{ (kips)}$$

(controlled by edge distance with the applied eccentricity factor)

B I B L I O G R A P H Y

1. Specification for the Design, Fabrication and Erection of Structural Steel for Buildings, American Institute of Steel Construction, New York, 1978.
2. Steel Structures for Buildings--Limit States Design, CSA Standard S16.1-1974, Canadian Standards Association, Rexdale, Ontario, 1974.
3. Specifications for Structural Joints Using ASTM A325 or A490 Bolts, Research Council on Riveted and Bolted Structural Joints, February 1976.
4. Fisher, J. W. and Struik, J. H., Guide to Design Criteria for Bolted and Riveted Joints, John Wiley and Sons, Inc., New York, 1974.
5. Price, K. D., "Behavior and Analysis of Bearing Critical Connections," unpublished Master's thesis submitted to the Faculty of Applied Science and Engineering, University of Toronto, April 1978.
6. Specification for the Design, Fabrication and Erection of Structural Steel for Buildings, American Institute of Steel Construction, New York, 1969.
7. Birkemoe, P. C. and Gilmor, M. I., Behavior of Bearing Critical Double Angle Beam Connections, Engineering Journal, American Institute of Steel Construction, Vol. 15, No. 4, 1978.
8. Kulak, G. L. and Crawford, S. F., Eccentricity Loaded Bolted Connections, Journal of the Structural Division, ASCE, Vol. 97, No. ST3, March 1971.
9. Higgins, T. R., New Formula for Fasteners Loaded Off Center, Engineering News Record, May 21, 1964.
10. Munse, W. H., Bell, W. G., and Chesson, Jr., E., Static Tests of Standard Riveted and Bolted Beam-to-Column Connections, University of Illinois Experimental Station Bulletin 146, Urbana, Illinois, January 1958.
11. American Society for Testing and Materials, Standard Methods of Tension Testing of Metallic Materials, ASTM Designation E8-79, Philadelphia, 1980.

12. American Society for Testing and Materials, Standard Methods and Definitions for Mechanical Testing of Steel Products, ASTM Designation A370-77, Philadelphia, 1980.
13. Stewart, W. C., "Determining Bolt Tension," Machine Design, Vol. 27, No. 11, New York, November 1955.
14. Wilson, E. L., Solid Sap: A Static Analysis Program for Three-Dimensional Solid Structures, Structural Engineering Laboratory University of California, Berkeley, September 1971.
15. Manual of Steel Construction, 7th Ed., American Institute of Steel Construction, New York, 1970.
16. Manual of Steel Construction, 8th Ed., American Institute of Steel Construction, New York, 1980.
17. Beam-to-Column Building Connections: State of the Art, Preprint 80-179, 1980 ASCE Spring Convention, Portland, 1980.
18. Shelton, B. G., "Tests of Bolted Shear Web Connections," unpublished Master's thesis, The University of Texas at Austin, December 1980.
19. Structural Steel Detailing, American Institute of Steel Construction, New York, 1971.

